

# Differential Regulation of Endosomal GPCR/ $\beta$ -Arrestin Complexes and Trafficking by MAPK\*

Received for publication, March 26, 2014, and in revised form, June 24, 2014. Published, JBC Papers in Press, July 11, 2014, DOI 10.1074/jbc.M114.568147

Etienne Khoury<sup>†1</sup>, Ljiljana Nikolajev<sup>§</sup>, May Simaan<sup>‡</sup>, Yoon Namkung<sup>‡</sup>, and Stéphane A. Laporte<sup>†§¶12</sup>

From the Departments of <sup>‡</sup>Medicine, <sup>§</sup>Pharmacology and Therapeutics, and <sup>¶</sup>Anatomy and Cell Biology, McGill University Health Center Research Institute, McGill University, Strathcona Anatomy & Dentistry Bldg., Quebec H3A 2B2, Canada

**Background:** Regulation between GPCRs and  $\beta$ -arrestins in endosomes has never been reported.

**Results:** A novel ERK regulatory site in  $\beta$ -arrestin-2 controls the binding to GPCRs in endosomes, and receptor trafficking and signaling.

**Conclusion:** Differential MAPK-dependent regulation of endosomal complexes exists among  $\beta$ -arrestin subtypes and species.

**Significance:** Such divergent mode of regulation may help understanding the physiological role of the endosomal GPCR/ $\beta$ -arrestins signaling axis.

$\beta$ -Arrestins are signaling adaptors that bind to agonist-occupied G protein-coupled receptors (GPCRs) and target them for endocytosis; however, the mechanisms regulating receptor/ $\beta$ -arrestin complexes and trafficking in endosomes, remain ill defined. Here we show, in live cells, differential dynamic regulation of endosomal bradykinin B2 receptor (B2R) complexes with either  $\beta$ -arrestin-1 or -2. We find a novel role for MAPK in the B2R/ $\beta$ -arrestin-2 complex formation, receptor trafficking and signaling mediated by an ERK1/2 regulatory motif in the hinge domain of the rat  $\beta$ -arrestin-2 (PET<sup>178P</sup>), but not rat  $\beta$ -arrestin-1 (PER<sup>177P</sup>). While the ERK1/2 regulatory motif is conserved between rat and mouse  $\beta$ -arrestin-2, it is surprisingly not conserved in human  $\beta$ -arrestin-2 (PEK<sup>178P</sup>). However, mutation of lysine 178 to threonine is sufficient to confer MAPK sensitivity to the human  $\beta$ -arrestin-2. Furthermore, substitution for a phosphomimetic residue in both the rat and the human  $\beta$ -arrestin-2 (T/K178D) significantly stabilizes B2R/ $\beta$ -arrestin complexes in endosomes, delays receptor recycling to the plasma membrane and maintains intracellular MAPK signaling. Similarly, the endosomal trafficking of  $\beta$ 2-adrenergic, angiotensin II type 1 and vasopressin V2 receptors was altered by the  $\beta$ -arrestin-2 T178D mutant. Our findings unveil a novel subtype specific mode of MAPK-dependent regulation of  $\beta$ -arrestins in intracellular trafficking and signaling of GPCRs, and suggest differential endosomal receptor/ $\beta$ -arrestin-2 signaling roles among species.

Heptahelical receptors such as G protein-coupled receptors (GPCRs)<sup>3</sup> are implicated in almost all physiological processes

\* This work was supported by Canadian Institutes of Health Research (CIHR) Operating Grants (to S. A. L.) (MOP-74603).

<sup>1</sup> Recipient of a studentship from the McGill Division of Endocrinology and Metabolism.

<sup>2</sup> Recipient of a Chercheur Boursier Senior scholarship from "Le Fonds de recherche du Québec - Santé" (FRQS). To whom correspondence should be addressed: Polypeptide Laboratory, McGill University, Strathcona Anatomy & Dentistry Bldg., 3640 University St., Room W315, Montreal, QC H3A 2B2, Canada. Tel.: 514-398-4487; Fax: 514-398-3923; E-mail: stephane.laporte@mcgill.ca.

<sup>3</sup> The abbreviations used are: GPCR, G protein-coupled receptor; AP-2, adaptor protein 2; AT1R, angiotensin II type 1; B2R, bradykinin B2 receptor;  $\beta$ 2AR,  $\beta$ 2-adrenergic receptor; FRAP, fluorescence recovery after photo-

including neurotransmission, metabolism, cardiovascular, and hormonal functions (1–3). Levels of GPCRs at the plasma membrane and their functional coupling to downstream signaling pathways, which contribute to these physiological responses are also intricately linked to  $\beta$ -arrestin functions.  $\beta$ -Arrestins are cytosolic proteins that terminate G protein-dependent signaling and act both as endocytic and signaling adaptors (4, 5). The arrestin family includes four members encoded by different genes (6): two visual arrestins (arrestin 1 and 4), which are confined to photoreceptors, and two non-visual ones,  $\beta$ -arrestin-1 and -2 (also commonly referred to as arrestin-2 and -3, respectively) that are expressed more ubiquitously and modulate the signaling and trafficking of many GPCRs. The current model for  $\beta$ -arrestin roles first requires the phosphorylation of agonist-bound receptors by dedicated GPCR kinases, and their recruitment to the phosphorylated GPCRs (7, 8).  $\beta$ -Arrestins will then serve as adaptors to link GPCRs to components of the endocytic machinery like clathrin and its adaptor protein 2 (AP-2), allowing receptors to internalize (4, 5, 9). Whether  $\beta$ -arrestins traffic inside the cells and complex with some receptors into endosomes or whether they dissociate from them at the plasma membrane during endocytosis, have also been used as criteria to typify GPCRs into different classes (10). For instance, Class A receptors, which usually display higher affinity for  $\beta$ -arrestin-2 than for  $\beta$ -arrestin-1, form short-lived complexes with both  $\beta$ -arrestins at the plasma membrane, internalize into endosomes without  $\beta$ -arrestins and are rapidly recycled to the plasma membrane. On the other hand, Class B receptors bind both  $\beta$ -arrestins with apparent similar affinities, form longer-lived complexes with  $\beta$ -arrestins into endosomes, and are generally retained for longer periods inside the cell, even if the ligand has been removed from the extracellular milieu. We have recently showed a hybrid trafficking behavior of  $\beta$ -arrestin with the bradykinin B2 receptor (B2R), a member of the GPCR family involved in the regulation of the renal and vascular functions. Similarly to class B receptors, B2R internalizes with  $\beta$ -arrestins into endosomes upon

bleaching; MEKDN, MEK-1 dominant negative; V2R, vasopressin V2 receptor.

agonist stimulation (11). However, these complexes are short-lived in endosomes, and receptors rapidly recycle back to the plasma membrane following agonist removal, hence more reminiscent of class A GPCRs in regards to such trafficking behavior. Whether, and if so, how receptor/ $\beta$ -arrestin complexes are regulated in endosomes for different GPCRs, and especially for B2R, still remains an open question.

$\beta$ -Arrestins also act as signaling adaptors. For example, they recruit Src kinases to receptors and assemble MAPK components such as Raf-1, MEK1, and ERK1/2 in endosomes, to promote signaling (12–14). Others and we have shown that the internalization of GPCRs through the clathrin pathway is also regulated by the scaffolding signaling functions of  $\beta$ -arrestins (15–18). For instance, phosphorylation of  $\beta$ -arrestin-1 by ERK1/2 in the C-terminal domain differentially modulates its ability to bind clathrin and AP-2, and impedes  $\beta$ 2-adrenergic receptor ( $\beta$ 2AR) internalization. The recruitment of Src kinase to receptor/ $\beta$ -arrestin-2 complexes allows the phosphorylation of the  $\beta$ -subunit of AP-2 and dynamin, which permits the internalization of the angiotensin II type 1 (AT1R) and the  $\beta$ 2AR (16, 19). Since we have shown that B2R/ $\beta$ -arrestin complexes recruit ERK1/2 (20), and given the important role of  $\beta$ -arrestins in scaffolding kinases to regulate GPCRs internalization, we sought to determine the extent to which MAPK participates in the  $\beta$ -arrestin-dependent trafficking of B2R. Because  $\beta$ -arrestin subtypes are highly conserved among species, it is often assumed that they share most cellular and physiological functions, despite that few studies have addressed such issues. Moreover, because the GPCR/ $\beta$ -arrestins signaling axis can be a potential therapeutic target, as recently demonstrated in different animal models such as rodents, we also compared  $\beta$ -arrestin 1 and 2 from rat and human in the  $\beta$ -arrestin-dependent MAPK regulation of different GPCR trafficking.

## EXPERIMENTAL PROCEDURES

**Materials**—DMSO was from Bioshop. PD98059 inhibitor was from Calbiochem. PD184352 and SP600125 inhibitors were from Sigma-Aldrich. Anti-HA antibody coupled to agarose beads and mouse anti-HA antibody (clone 12CA5) were purchased from Roche (Laval, Canada). The polyclonal antibody against the C-terminal domain of  $\beta$ -arrestins, BARR3978 was described elsewhere (21). Mouse monoclonal anti-phospho-ERK1/2 (T202/Y204) and rabbit polyclonal anti-total ERK1/2 were from Cell Signaling Technology (Danvers, MA). Anti-mouse and anti-rabbit HRP-conjugated IgG were from Sigma-Aldrich and the chemiluminescence lightening (ECL) was from Perkin-Elmer. MEM and DMEM were from Hyclone (Logan, UT). Fetal bovine serum (FBS), L-glutamine and gentamicin were purchased from Invitrogen (Carlsbad, CA), and zeocin was from Invivogen (San Diego, CA). Dithiobis succinimidyl propionate (DSP) was from Pierce. Phenylmethyl sulfonyl fluoride (PMSF), aprotinin, leupeptin, and pepstatin were from Bioshop (Burlington, Canada).

**Plasmids and Constructs**—Plasmids encoding HA-B2R, HA-AT1R, HA-V2R, HA- $\beta$ 2AR, B2R-YFP, human  $\beta$ -arrestin-2-YFP, rat  $\beta$ -arrestin-1-YFP, and  $\beta$ -arrestin-2-myc have been previously described elsewhere (20–23). Dynamin K44A was described in Zhang *et al.* (24). Rat  $\beta$ -arrestin-2-YFP construct

was cloned into pEYFP-N1 using HindIII and KpnI sites. The rat  $\beta$ -arrestin-2-YFP T178K, T178A, and T178D constructs were generated by PCR using a forward primer overlapping the HindIII site in 5'-prime and a reverse primer for introducing either a lysine, an alanine or an aspartic acid residue at position 178, and for creating an internal ApaI site. Another PCR was also generated using a forward primer overlapping the ApaI site and a reverse primer overlapping the KpnI site. The vector pEYFP-N1 was cut with HindIII and KpnI, and the two PCR products of each construct were three-way ligated with the digested vector. A similar strategy was also employed for generating the human  $\beta$ -arrestin-2-YFP K178T and K178D, with the exception of that the PCR products were cloned into pEYFP-N1 cut with HindIII and BamHI. The rat  $\beta$ -arrestin-2 S265A/T277A was generated by overlapping PCR. First, a PCR fragment was generated using a forward primer overlapping the HindIII site in 5'-prime with a reverse primer overlapping the BlnI, and second one using a forward primer overlapping BlnI including both mutations (S265A/T277A) with a reverse primer overlapping the KpnI site. Using these PCR fragments as a template, another PCR product was generated using a forward primer overlapping the HindIII site in 5'-prime and a reverse primer overlapping the KpnI site. The vector pEYFP-N1 was cut with HindIII and KpnI, and the final PCR product was ligated into the digested vector. For generating the rat  $\beta$ -arrestin-2-T178D Myc-tagged construct, a 5'-prime fragment of the rat  $\beta$ -arrestin-2-YFP-T178D was cut with HindIII and BlnI, and three-way ligated with a BlnI/SalI 3'-prime fragment in the pCMV-3Tag-2A vector previously digested with HindIII and SalI. Human MEK1 cDNA was provided by Dr. J. Charron (Université Laval, Québec, Canada). For the Flag-tagged MEK construct (MEKWT), the cDNA was cloned into pCMV-Tag using the BamHI/EcoRI sites. The MEK K97A-Flag (MEKDN) was generated by replacing a BamHI/BspEI fragment from the MEK-Flag construct with a PCR fragment generated with a T3 forward primer and a 3'-prime reverse primer overlapping the Lys 97 codon (substituting the Lys for an Ala residue) and the BspEI, cut with the same enzymes. Red fluorescent-fused proteins (RFP) of MEK were generated from MEKWT-Flag and MEKDN-Flag sequences by PCR using a forward primer overlapping the HindIII site (omitting the Flag sequence) and a reverse primer overlapping the stop codon and creating a KpnI site. PCR products were then cloned in frame into mRFP-C1 cut with the same enzymes. All constructs were analyzed by DNA sequencing (Sequencing Service, Genome Quebec Innovation Centre, McGill University, QC, Canada).

**Cell Culture and Transfection**—Stable human embryonic kidney (HEK) 293 cells expressing the B2R receptor (HEK293-B2R cells) were generated by transfecting the HA-tagged B2R cloned into pcDNA3.1/Zeo(+) (Invitrogen™). Cells were then selected in 0.7  $\mu$ g/ml zeocin, and expression levels were validated from radio-ligand binding assays (see below). Expression levels of receptor were found to be around 250 fmol/mg of total cell protein (*i.e.*  $\approx$ 75,000 receptors/cell). HEK293 cells were grown at 37 °C in 5% CO<sub>2</sub> in MEM supplemented with 10% (*v/v*) heat-inactivated fetal bovine serum and gentamicin (100  $\mu$ g/ml). Cells were seeded at densities of 4  $\times$  10<sup>5</sup> cells per 100-mm dish or at 1  $\times$  10<sup>5</sup> cells per 35-mm dish, and trans-

## Endosomal Signaling Function of $\beta$ -Arrestin on GPCR Trafficking

ected using conventional calcium phosphate co-precipitation methods. COS-7 cells were grown in DMEM (Invitrogen) supplemented with 10% (*v/v*) heat-inactivated fetal bovine serum (FBS) and 100  $\mu\text{g/ml}$  gentamicin (Invitrogen<sup>™</sup>). Transfection of COS-7 cells that were seeded in 100-mm dish at a density of  $8 \times 10^5$  cells per 100-mm dish or  $8 \times 10^4$  per well in a 24-well plate was performed using Lipofectamine 2000 (Invitrogen<sup>™</sup>) according to the manufacturer's recommendations using 1:2 ratio of DNA:Lipofectamine in Opti-MEM (Invitrogen<sup>™</sup>). All experiments were performed 48 h post-transfection.

**Confocal Microscopy Experiments**—HEK293 cells were seeded in 35-mm glass bottom dishes (MaTek Corp., Ashland, MA) and transfected with HA-B2R and either the YFP-tagged rat  $\beta$ -arrestin-2 or mutants (T178K, S265A/T277A, T178A, and T178D), or the YFP-tagged human  $\beta$ -arrestin-2 or mutants (K178T and K178D). For experiments with the HA-vasopressin V2 receptor (V2R), HA- $\beta$ 2AR, and HA-AT1R, receptors were individually expressed in HEK293 cells with either the YFP-tagged rat  $\beta$ -arrestin-2 or the T178D mutant. For assessing MAPK activity, HEK293 cells were transfected with HA-B2R and the rat  $\beta$ -arrestin-2-YFP and either MEKWT-Flag or MEKDN-Flag. Forty-eight hours post-transfection, cells were serum starved for 30 min followed by stimulation with bradykinin, vasopressin, isoproterenol, or angiotensin II (1  $\mu\text{M}$ ) for 15 min. For pharmacological MEK inhibition, cells were treated with either DMSO (vehicle), PD98059 (20  $\mu\text{M}$ ), PD184352 (20  $\mu\text{M}$ ), or SP600125 (20  $\mu\text{M}$ ) for 30 min before bradykinin stimulation and fluorescence recovery after photobleaching (FRAP) experiments were performed. FRAP was applied on endosomes containing  $\beta$ -arrestin-YFP as previously described (23, 25). Briefly, endosomes from at least eleven to twenty four independent experiments were individually bleached, and fluorescence recovery was monitored over a period of 3 min with image acquisition every 30 s. Regions of interest (ROI) were bleached for 100 iterations using a 514 nm Argon laser set at 100% intensity on a Zeiss LSM-510 Meta laser scanning microscope with a 63 $\times$  oil immersion lens. Images (1024  $\times$  1024 pixels) were then collected using an emission BP 530–600 nm filter. For detecting mRFP, a HeNe I laser was used with 543 nm excitation and LP 560 nm emission filter sets. Fluorescence intensity data were converted into a linear regression plot to obtain maximal recovery as described previously (23, 25) and expressed as percentage recovery (%) / time (s) in function of fluorescence recovery (%) using GraphPad Prism 4. To compare endosomal  $\beta$ -arrestin half-life recovery between experiments, maximal recovery after 3 min was fixed at 100% for each condition. Endosomes of similar size and intensity were used in all experiments.

For quantification of the number of endosomes containing B2R, HEK293 cells were seeded in 35-mm glass bottom dishes and transfected with B2R-YFP and  $\beta$ -arrestin-2-myc. Forty-eight hours post-transfection, cells were serum starved for 30 min, treated with either DMSO (vehicle) or PD98059 (20  $\mu\text{M}$ ) for another 30 min, before bradykinin stimulation. After endosomal formation, as detected by the fluorescence of B2R-YFP, the total number of endosomes with diameters  $>1 \mu\text{m}$  were counted using Image J software and expressed over cell surface.

Ratios were calculated from three independent experiments, comparing DMSO- to PD98059-treated cells.

For recycling experiments, HEK293 cells were seeded in 35-mm glass bottom dishes and transfected with B2R-YFP and either myc-tagged  $\beta$ -arrestin-2 or the T178D mutant. For MEK inhibition, cells were also transfected with either MEKWT-mRFP or MEKDN-mRFP, and treating cells with either DMSO (vehicle), PD98059 (20  $\mu\text{M}$ ), or PD184352 (20  $\mu\text{M}$ ) for 30 min before bradykinin stimulation. Forty-eight hours post-transfection, cells were serum starved for 30 min followed by stimulation with bradykinin (1  $\mu\text{M}$ ) for 15 min. After the appearance of B2R-YFP in endosomes, cells were washed three times with MEM medium to remove cell surface-bound ligand, and images (1024  $\times$  1024 pixels) of receptor were acquired for 40 min using conditions described for YFP detection.

**Immunoprecipitation and Western Blot Experiments**—Co-immunoprecipitation of covalently cross-linked  $\beta$ -arrestin-2-YFP to HA-B2R was performed as previously described (11). Briefly, either COS-7 cells or HEK293-B2R cells were seeded at a density of  $8 \times 10^5$  per 100 mm dish, then transfected the second day with HA-B2R and  $\beta$ -arrestin-2-YFP, and either MEKWT-Flag or MEKDN-Flag. Forty-eight hours post transfection, cells were serum starved as described previously and challenged with bradykinin (1  $\mu\text{M}$ ) for 15 min. For pharmacological MEK inhibition, cells were first treated with either DMSO (vehicle) or PD98059 (20  $\mu\text{M}$ ) for 30 min after being serum starved, and then stimulated with bradykinin (1  $\mu\text{M}$ ) for 15 min. Agonist stimulation was stopped following the addition of DSP at a final concentration of 2 mM. Cells were then washed with PBS containing 50 mM Tris-HCl to neutralize DSP, and lysed in a glycerol buffer containing 100  $\mu\text{M}$  sodium orthovanadate, 1 mM phenylmethylsulfonyl fluoride, 25  $\mu\text{g/ml}$  leupeptin, 2.5  $\mu\text{g/ml}$  aprotinin, and 1 mM pepstatin. Cell lysates were cleared by centrifugation (14,000 rpm for 30 min), and the supernatants were incubated overnight with monoclonal anti-HA affinity agarose beads (Roche). Beads were then washed with glycerol buffer and denatured in Laemmli buffer. Samples were run on 10% SDS-PAGE, and Western blotting was performed using anti-HA (12CA5) and anti- $\beta$ -arrestin antibodies (BARR3978), and anti-phospho-ERK1/2. Immunoreactivity was visualized by enhanced chemiluminescence according to the manufacturer's instructions (Perkin Elmer).

**Radioligand Binding Assay**—Ligand binding assay was performed as described previously with minor modifications (11). Briefly, COS-7 cells were seeded at a density of  $8 \times 10^5$  cells in 100-mm dishes and transfected with HA-B2R and either  $\beta$ -arrestin-2 WT or T178D. The next day, cells were transferred into 24-well plates at a density of  $8 \times 10^4$  cells per well. In recycling experiments, after bradykinin stimulation (50 nM, 15 min), cells were washed with prewarmed medium to remove surface bound ligand, and then were kept at 37  $^{\circ}\text{C}$  for the indicated time to allow receptor recycling. Incubation was immediately stopped by putting plates on ice, and cells were rapidly washed three times (5 min each time) with ice-cold acid buffer (50 mM sodium citrate, 90 mM NaCl, pH 4.0) followed by one ice-cold PBS wash to remove both the unbound and the cell surface receptor bound agonist. Cells were then incubated with cold binding buffer (50 mM Tris-HCl, 1 mM captopril, 1 mM phenanthroline-1,10, and 140  $\mu\text{g/ml}$  bacitracin, pH 7.4 at 4  $^{\circ}\text{C}$ ) and

1.28 nM of  $^{125}\text{I}$ -[Tyr<sup>8</sup>]bradykinin (1000 Ci/mmol) in a total volume of 0.5 ml, and kept overnight at 4 °C. The next day, cells were washed three times with ice-cold PBS then solubilized with 0.5 ml of 0.5 M NaOH and 0.05% sodium dodecyl sulfate (w/v), and radioactivity was assessed using a gamma-counter. Nonspecific binding was measured in the presence of 1  $\mu\text{M}$  of unlabeled bradykinin. Percent of receptor internalization and recycling was calculated from the ratio of treated over non-treated conditions as described previously (11).

**MAPK Assay**—COS-7 cells were seeded in a 6-well plate at a density of  $1 \times 10^5$  cells/well and transfected with HA-B2R and either the YFP-tagged rat  $\beta$ -arrestin-2 WT or the T178D mutant, or with the YFP-tagged human  $\beta$ -arrestin-2 WT or the K178D mutant. Forty-eight hours post-transfection, cells were serum starved for 30 min in DMEM containing 20 mM HEPES, and then left either untreated or treated with bradykinin (1  $\mu\text{M}$ ) for the indicated time. Treatment was stopped on ice with cold PBS, and cells were solubilized in 2 $\times$  Laemmli buffer (250 mM Tris-HCl pH 6.8, 2% SDS (w/v), 10% glycerol (v/v), 0.01% bromophenol blue (w/v), and 5%  $\beta$ -mercaptoethanol (v/v)). Lysates were resolved on a 10% SDS-PAGE and analyzed by Western blot using anti-phospho-ERK1/2, anti-total-ERK1/2, and anti- $\beta$ -arrestin antibody (BARR3978).

**Statistical Analysis**—Signals from Western blots were determined by densitometry analysis using Image J, and are presented as the mean  $\pm$  S.E. of at least three independent experiments. Statistical analysis was performed with Graphpad Prism software using *t* tests or two-way ANOVA when appropriate. Bonferroni (comparison between all groups) post-tests were performed where necessary.

## RESULTS

**MAPK Regulates B2R/ $\beta$ -arrestin-2 Complexes in Endosomes and Receptor Trafficking**—Because  $\beta$ -arrestins act as signaling scaffolds, and because signaling through  $\beta$ -arrestins regulates endocytic complex assembly during the internalization of GPCRs (15, 16, 21), we first tested the role of MAPK signaling on B2R/ $\beta$ -arrestin interaction and receptor trafficking. To this end, we expressed HA-tagged B2R with either the murine  $\beta$ -arrestin-1-YFP or  $\beta$ -arrestin-2-YFP in HEK-293 cells (Fig. 1). Cells were then treated with either DMSO (vehicle) or 20  $\mu\text{M}$  of MEK inhibitor PD98059, which inhibited ERK1/2 activation (Fig. 2A), before being challenged with bradykinin for 15 min to allow receptor internalization and the formation of B2R/ $\beta$ -arrestin complexes in endosomes. To monitor the lifetime of B2R/ $\beta$ -arrestin complexes in endosomes, we assessed in real time the fluorescence recovery of YFP-labeled  $\beta$ -arrestins onto endosomes using a fluorescence recovery after photobleaching (FRAP) method. The recovery of  $\beta$ -arrestins-YFP onto the endosomes from a surrounding cytosolic pool is dependent on the strength of the interaction between the receptor and the bleached  $\beta$ -arrestins-YFP. It is inversely proportional to the stability of the complex (26), hence, if the interaction between  $\beta$ -arrestin and a receptor is labile, this exchange and the recovery of fluorescence will be faster, and vice versa. Results showed that the fluorescence recovery of  $\beta$ -arrestin-1-YFP onto endosomes containing B2R occurred more rapidly than for  $\beta$ -arrestin-2-YFP (Fig. 1, A and C, respectively). Indeed, quantification

reveals that fluorescence half-time recovery was around three times faster for  $\beta$ -arrestin-1 than for  $\beta$ -arrestin-2 ( $42.90 \pm 5.7$  and  $123.40 \pm 9.1$  s, respectively; Fig. 2E). Treating cells with the MEK inhibitor PD98059 significantly decreased the recovery time of  $\beta$ -arrestin-2 to endosomes by  $\sim 50\%$  ( $123.40 \pm 9.1$  s to  $65.99 \pm 9.2$  s; Figs. 1, C and D, and 2E), while it had no significant effect on  $\beta$ -arrestin-1 recovery rates (Figs. 1, A and B, and Fig. 2E). Similarly, expression of a dominant negative form of MEK-1 (MEKDN), which impedes receptor-mediated ERK1/2 activation, also significantly decreased by more than 40% the recovery time of  $\beta$ -arrestin-2-YFP ( $139.10 \pm 13.0$  s to  $79.81 \pm 7.2$  s; Figs. 1, E and F, and 2E). Other MAPK inhibitors were also tested on the endosomal complex formation. Results show that while the other MEK inhibitor PD184352 significantly decreased the recovery time of  $\beta$ -arrestin-2 on endosomes to half times similar to that of PD98059 (*i.e.* reduction of 45%; Fig. 2, A, B, and E), the JNK inhibitor SP600125 (Fig. 2C) had no significant effect on the receptor/ $\beta$ -arrestin-2 interaction when compared with DMSO treated cells (Fig. 2, D and E). Because ERK1/2 is found in a complex in endosomes with both  $\beta$ -arrestin-2 and B2R (20), we next wanted to confirm biochemically the effect of inhibiting MAPK on such complex formation. In cells challenged with bradykinin for 15 min, we observed a 40% decreased association between  $\beta$ -arrestin-2 and the immunoprecipitated B2R when cells were either treated with PD98059 (Fig. 3, A and B) or transfected with MEKDN (Fig. 3, C and D), as compared with control cells.

The dissociation of  $\beta$ -arrestins from B2R in endosomes is required for receptor recycling at the plasma membrane (11). We next sought to know how reducing the avidity of B2R/ $\beta$ -arrestin-2 complex in the endosomes by inhibiting MAPK impacted recycling of receptors. HEK293 cells were transfected with B2R-YFP and Myc-tagged  $\beta$ -arrestin-2, and cells were stimulated with bradykinin for 15 min to allow receptor internalization. We observed the formation of many large endosomes containing B2R, whereas cells pre-treated with the PD98059 and challenged with bradykinin showed qualitatively smaller (Fig. 4A, *middle panel*), and quantitatively lesser endosomes containing receptors (Fig. 4B). When bradykinin was then removed from the milieu by washing to allow receptor recycling, we observed some regain of B2R signal at the plasma membrane in control conditions (DMSO-treated cells; Fig. 4A, *bottom panel*), but the presence of receptor-labeled endosomes was still obvious. However, the disappearance of the fluorescence in the endosomes and the regain of receptor at the plasma membrane were more noticeable in cells treated with either PD98059 or PD184352 (Fig. 4A, *left and right bottom panels*, respectively). Similarly, at 40 min post-ligand wash (Fig. 4C *bottom panels*), we observed that the disappearance of B2R from large endosomes and the recycling of the receptor at plasma membrane was more obvious in cells transfected with MEKDN than for control cells expressing wild type MEK. Interestingly, the remaining B2R in endosomes in MEKDN expressing cells following bradykinin removal, were found in smaller vesicles compared with those observed in the control cells. Taken together, these results suggest that the MEK-ERKs signaling axis plays an important role in regulating

## Endosomal Signaling Function of $\beta$ -Arrestin on GPCR Trafficking

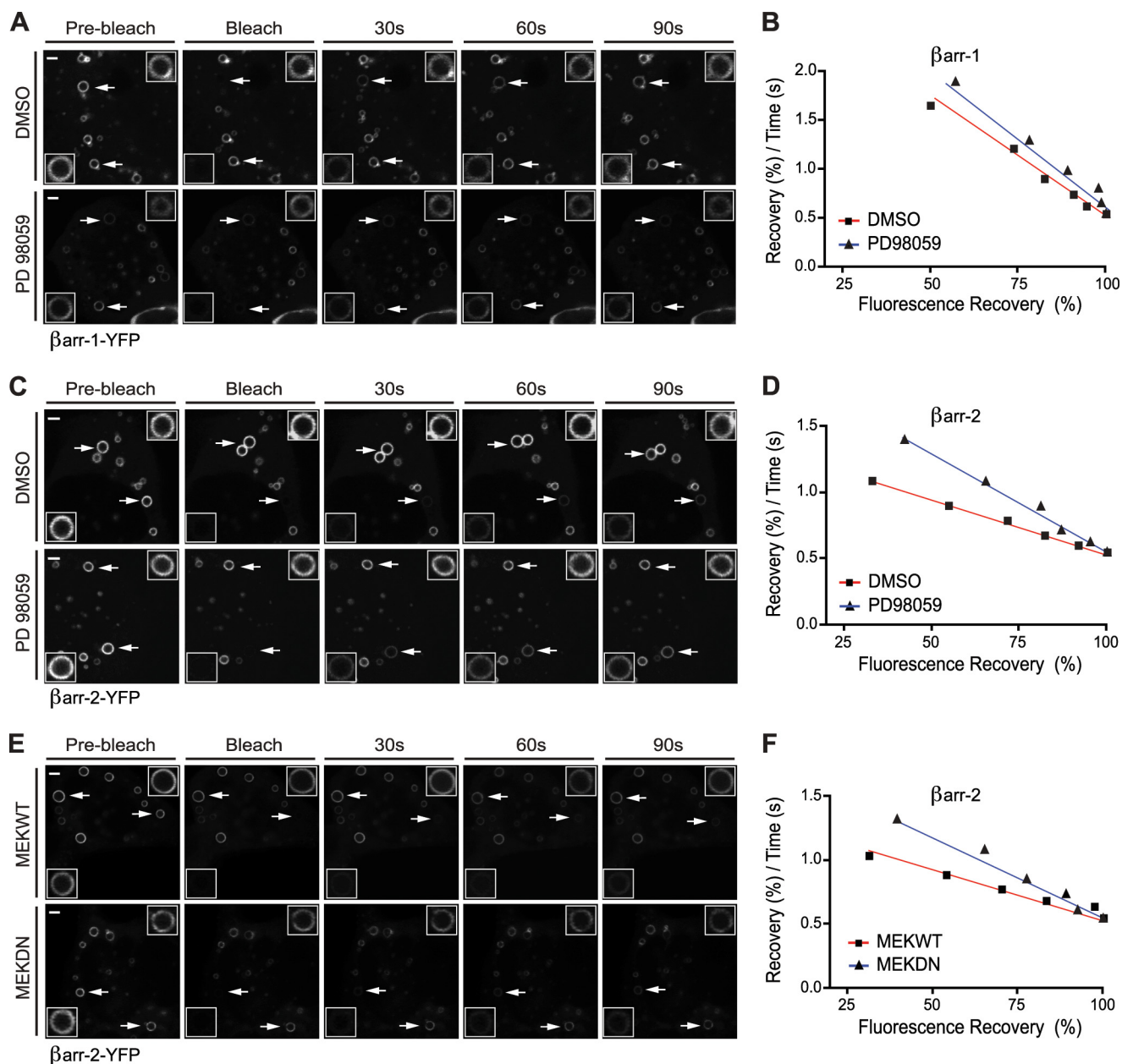


**FIGURE 1. Inhibition of MAPK reduces the lifetime of B2R/ $\beta$ -arrestin-2 complexes in endosomes.** A and C, representative images of FRAP experiments on endosomes from HEK293 cells expressing HA-B2R and either (A),  $\beta$ -arrestin1-YFP ( $\beta$ arr-1-YFP), or (C),  $\beta$ -arrestin-2-YFP ( $\beta$ arr-2-YFP). Cells were either left untreated (DMSO) or treated with PD98059 (20  $\mu$ M, 30 min), before being challenged with bradykinin (1  $\mu$ M, 15 min) as indicated in "Experimental Procedures." Endosomes containing B2R and  $\beta$ -arrestins were selected (white arrows), and either bleached (bottom insets) or left unbleached (top insets). Fluorescence was then monitored over time every 30 s (30, 60, 90 s). E, representative images of FRAP experiments on endosomes containing the  $\beta$ -arrestin-2-YFP, and transfected with either MEKWT or MEKDN. B, D, and F, linear regression analysis of the recovery rates of  $\beta$ -arrestins onto endosomes containing B2R from panels A, C, and E, respectively. Scale bars are 10  $\mu$ m.

endosomal B2R/ $\beta$ -arrestin-2 interaction and intracellular receptor trafficking.

**Identification of a Novel MAPK-dependent Regulatory Site in the Hinge Domain of  $\beta$ -Arrestin-2**—Because MAPK inhibition affected the endosomal interaction between B2R and  $\beta$ -arrestin-2, but not with  $\beta$ -arrestin-1, we sought to identify differences in their sequences that would explain such distinct susceptibility. Analysis of  $\beta$ -arrestin-2 sequence identified three putative ERK phosphorylation sites in its sequence (e.g. S/TP: Thr<sup>178</sup>, Thr<sup>277</sup>, and Ser<sup>265</sup> with scores of 2.096, 1.096, and 0.352, respectively) (Fig. 5A). Only two of these residues are not con-

served between the two subtypes (Thr<sup>178</sup>, and Ser<sup>265</sup>), potentially excluding *de facto* Thr<sup>277</sup> as the regulatory site. However, we substituted both Thr<sup>277</sup> and Ser<sup>265</sup> residues at once for Ala (S265A and T277A) to exclude any participation of these two sites with the lowest phosphorylation scores. The half-time recovery of the  $\beta$ -arrestin-2 mutant onto the endosomes was still significantly decreased by more than 60% with PD98059 treatment (Fig. 5, C and E), suggesting that these residues are not the main targets of MAPK for regulating the receptor/ $\beta$ -arrestin-2 interaction in endosomes. Thr<sup>178</sup> is part of the well conserved P-E-T/S-P motif and only found in the hinge domain

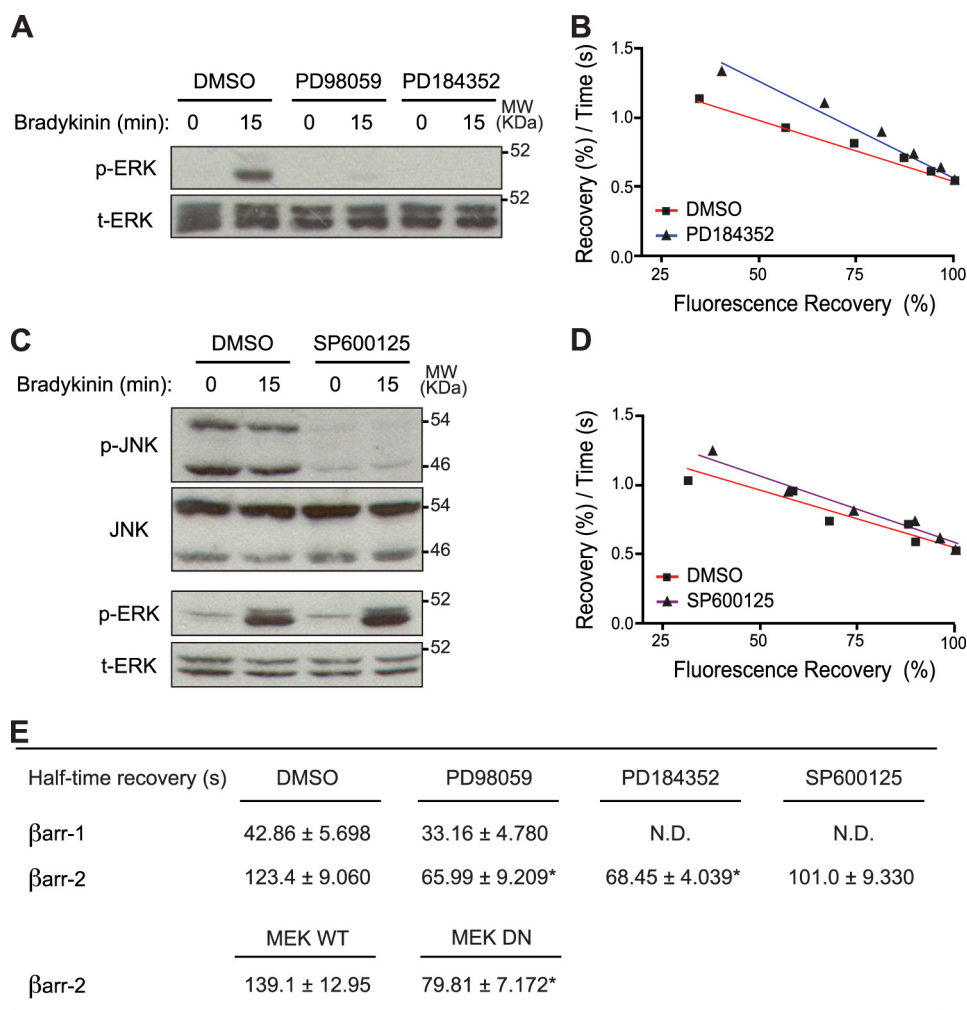


**FIGURE 2. Inhibition of ERK1/2 activity decreases the life-time of B2R/ $\beta$ -arrestin-2 complex in endosomes.** *A* and *C*, shown are representative immunoblots of ERK1/2 and JNK phosphorylation from HEK293 cells expressing HA-B2R and  $\beta$ -arrestin-2-YFP. Cells were either left untreated (DMSO), treated with (A) PD98059, PD184352 (20  $\mu$ M, 30 min), or (C) SP600125 (20  $\mu$ M, 30 min), then challenged with bradykinin (1  $\mu$ M) for 15 min. Lysates were immunoblotted for phosphorylated ERK (p-ERK), total ERK (t-ERK), phosphorylated JNK (p-JNK), and total JNK (JNK). Molecular markers of 46, 52, and 54 kDa are depicted. *B* and *D*, FRAP analysis is presented as regression plots and was performed in HEK293 cells transiently transfected with HA-B2R and  $\beta$ -arrestin-2-YFP after 15 min of bradykinin stimulation (1  $\mu$ M), and either DMSO, (B) PD184352 (20  $\mu$ M, 30 min), or (D) SP600125 (20  $\mu$ M, 30 min) treatments as described in "Experimental Procedures." *E*, shown are half-time recovery (s) data of  $\beta$ -arrestin-1 ( $\beta$ arr-1) and  $\beta$ -arrestin-2 ( $\beta$ arr-2) on endosomes containing B2R, calculated from the linear regression analysis presented in Figs. 1, *B*, *D*, and *F* and 2, *B* and *D*. Statistical analysis were performed by using Student's *t* test; \*,  $p < 0.05$ . Data are the mean  $\pm$  S.E. for 14–23 endosomes per condition. *N.D.*, not determined.

of  $\beta$ -arrestin-2 (Fig. 5, *A* and *B*) (27, 28). Replacing Thr<sup>178</sup> for an Ala residue abolished the effect of PD98059 treatment on the receptor/ $\beta$ -arrestin-2 complex half-life (Fig. 5, *D* and *E*). Because Thr<sup>178</sup> seems to be the regulatory site, we next substituted it for an Asp residue to mimic a negative charge resulting for its phosphorylation, and then assessed the endosomal B2R/ $\beta$ -arrestin-2 complex formation. FRAP results showed that introducing such negative charge in the  $\beta$ -arrestin-2 significantly increased the stability of the complex in endosomes because the recovery rates of the mutant was significantly slowed down, with half-time recovery that increased by more than 2-fold as compared with wild-type  $\beta$ -arrestin-2 (Fig. 6, *A*, *B*, and *C*). Such effect on the increased B2R/ $\beta$ -arrestin-2 complex formation was also validated biochemically (Fig. 6, *D* and *E*).

*The Hinge Domain of  $\beta$ -Arrestin-2 Regulates Endosomal Interactions with Other GPCRs and Receptor Trafficking*—We next assessed to what extent mimicking Thr<sup>178</sup> phosphorylation affected the endosomal interaction of  $\beta$ -arrestin-2 with

either class B GPCRs like the V2R and the AT1R, or a class A receptor, such as the  $\beta$ 2AR. Expressing  $\beta$ -arrestin-2 T178D in cells significantly increased by more than 2.4-fold the half-life of complexes between V2R and  $\beta$ -arrestin-2 compared with wild type (Fig. 7, *A* and *B*). The half-time recovery of  $\beta$ -arrestin-2 T178D to V2R in endosomes became comparable to that of wild type  $\beta$ -arrestin-2 with AT1R. Moreover, the recovery rate of the phospho-mimic  $\beta$ -arrestin-2 mutant on the AT1R-containing endosomes was also increased by 1.4-fold (Fig. 7*B*). For the  $\beta$ 2AR, we observed the accumulation of  $\beta$ -arrestin-2 T178D in endosomes following agonist stimulation (Fig. 7*C*). This contrasted with wild type  $\beta$ -arrestin, which, as we showed previously, can be recruited at the plasma membrane upon agonist activation of  $\beta$ 2AR, but does not internalize into endosomes with the receptor (29, 30). The endosomes containing  $\beta$ -arrestin-2 T178D were smaller and more labile than the ones observed with class B receptors, which prevented us from performing FRAP quantifications. Together, our findings imply

## Endosomal Signaling Function of $\beta$ -Arrestin on GPCR Trafficking

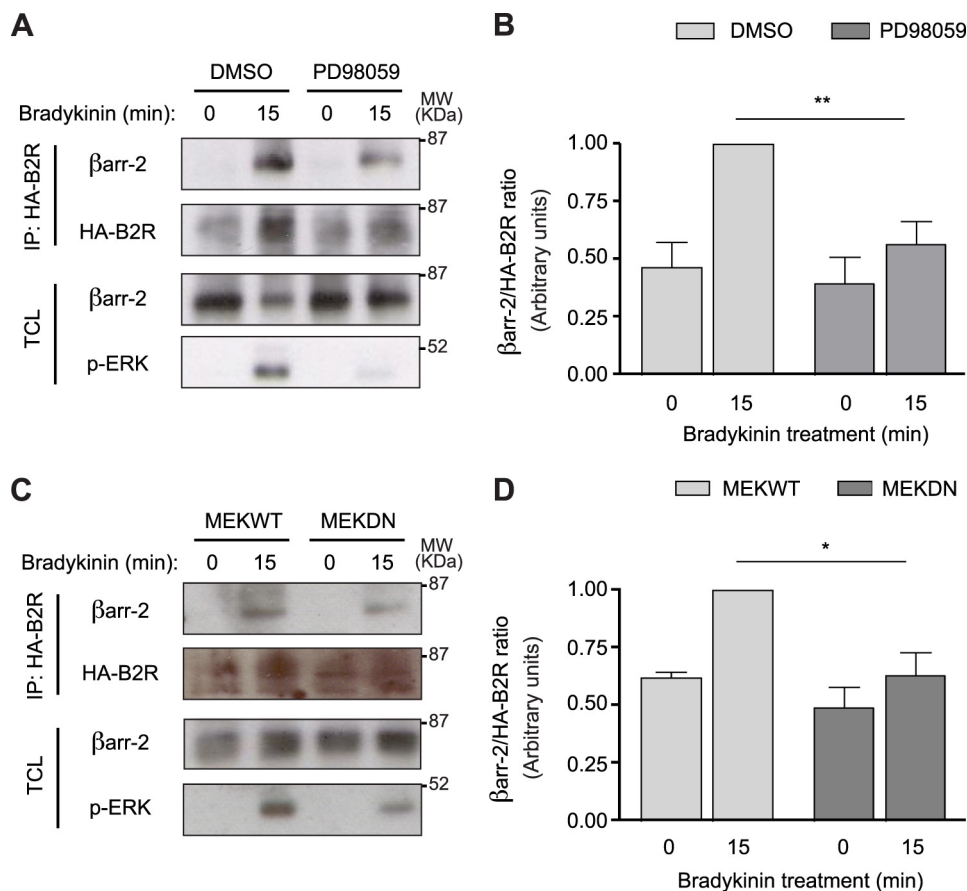


**FIGURE 3. MAPK inhibition reduces B2R/ $\beta$ -arrestin-2 complex formation.** COS-7 cells expressing HA-B2R and  $\beta$ -arrestin-2 were (A) either treated with DMSO, with PD98059 (20  $\mu$ M, 30 min), or (C) transfected with MEKWT or MEKDN before being challenged with bradykinin (1  $\mu$ M, 15 min). Lysates from immunoprecipitated (IP) HA-B2R were analyzed by Western blot using anti-HA (12CA5) and a  $\beta$ -arrestin antibody (BARR3978) for receptor and  $\beta$ -arrestin-2 detection, respectively. Total cell lysates (TCL) were blotted for  $\beta$ -arrestin-2 and p-ERK. Shown are representative blots of (A) five and (C) three independent experiments. Molecular markers of 52 and 87 kDa are presented. *B* and *D*, densitometry analysis of immunoprecipitation experiments. Data represent the relative expression of  $\beta$ -arrestin-2 normalized to the amounts of HA-B2R, as compared with the 15 min bradykinin stimulation, which is set at a 100% of (A) DMSO and (C) MEKWT conditions. Densitometry results are presented as the mean  $\pm$  S.E. Statistical significance was analyzed by a two-way ANOVA followed by a Bonferroni post-test. \*,  $p < 0.05$ ; \*\*,  $p < 0.01$ .

that the  $\beta$ -arrestin-2 hinge is important for its high affinity interaction with GPCRs.

We next investigated how  $\beta$ -arrestin-2 T178D affected recycling of the B2R. Binding assays were performed in cells after bradykinin stimulation, and receptor levels at the plasma membrane were evaluated 5, 15, and 30 min after removing the ligand to allow receptor recycling. Results show that B2R recycling decreased by around 50% in conditions where  $\beta$ -arrestin-2 phospho-mimic mutant was expressed, as compared with wild type  $\beta$ -arrestin-2-transfected cells (Fig. 8A). These findings were also supported by microscopy. We qualitatively observed less receptors trafficking back at the plasma membrane after ligand removal in cells expressing  $\beta$ -arrestin-2 T178D than in those expressing wild-type  $\beta$ -arrestin-2 (Fig. 8B). Consistent with the lack of receptor recycling to the plasma membrane, the B2R/ $\beta$ -arrestin-2 T178D complexes migrated to larger perinuclear endosomes, while WT complexes were found in smaller recycling endosomes.

**Differential Endosomal Signaling Roles between Human and Rat  $\beta$ -Arrestin-2**—Threonine 178 in the hinge domain is present in many rodent  $\beta$ -arrestin-2 subtypes, but is replaced for a positive charge (Lys<sup>178</sup>) in many other mammals like the human

and bovine orthologs (Fig. 9A), suggesting that the regulation of endosomal  $\beta$ -arrestin/receptor complexes differs among species. We thus tested the effects of inhibiting MAPK on the lifetime interaction between human  $\beta$ -arrestin-2 and B2R. The half-time recovery of the human  $\beta$ -arrestin-2 (h $\beta$ arr-2) on the endosome following photobleaching was 1.7 times faster than with rat  $\beta$ -arrestin-2 (r $\beta$ arr-2) (73.55  $\pm$  4.5 s versus 123.40  $\pm$  9.1 s, respectively), but 1.7 times slower than for rat  $\beta$ -arrestin-1 (r $\beta$ arr-1) (73.55  $\pm$  4.5 s versus 42.86  $\pm$  5.7s, respectively) (Figs. 9F and 2E). Moreover, recovery rates of the human  $\beta$ -arrestin-2 onto endosomes were not affected by MAPK inhibition (Fig. 9, B and F). To further validate the role of this regulatory site on the  $\beta$ -arrestin/B2R, we generated a gain-of-function  $\beta$ -arrestin-2 by introducing a Threonine into the human ortholog ( $\beta$ -arrestin-2 K178T); and vice versa, generated a loss-of-function mutant by replacing the one in rat  $\beta$ -arrestin-2 by the analogous residue in the human  $\beta$ -arrestin-2 (T178K), and assessed the dynamic regulation of the complex in endosomes by FRAP. Reconstituting the putative ERK phosphorylation site into the human  $\beta$ -arrestin-2 (K178T) significantly increased its time of recovery onto endosomes by almost 35% as compared with WT (Fig. 9, C and F), which half-time recovery was now comparable

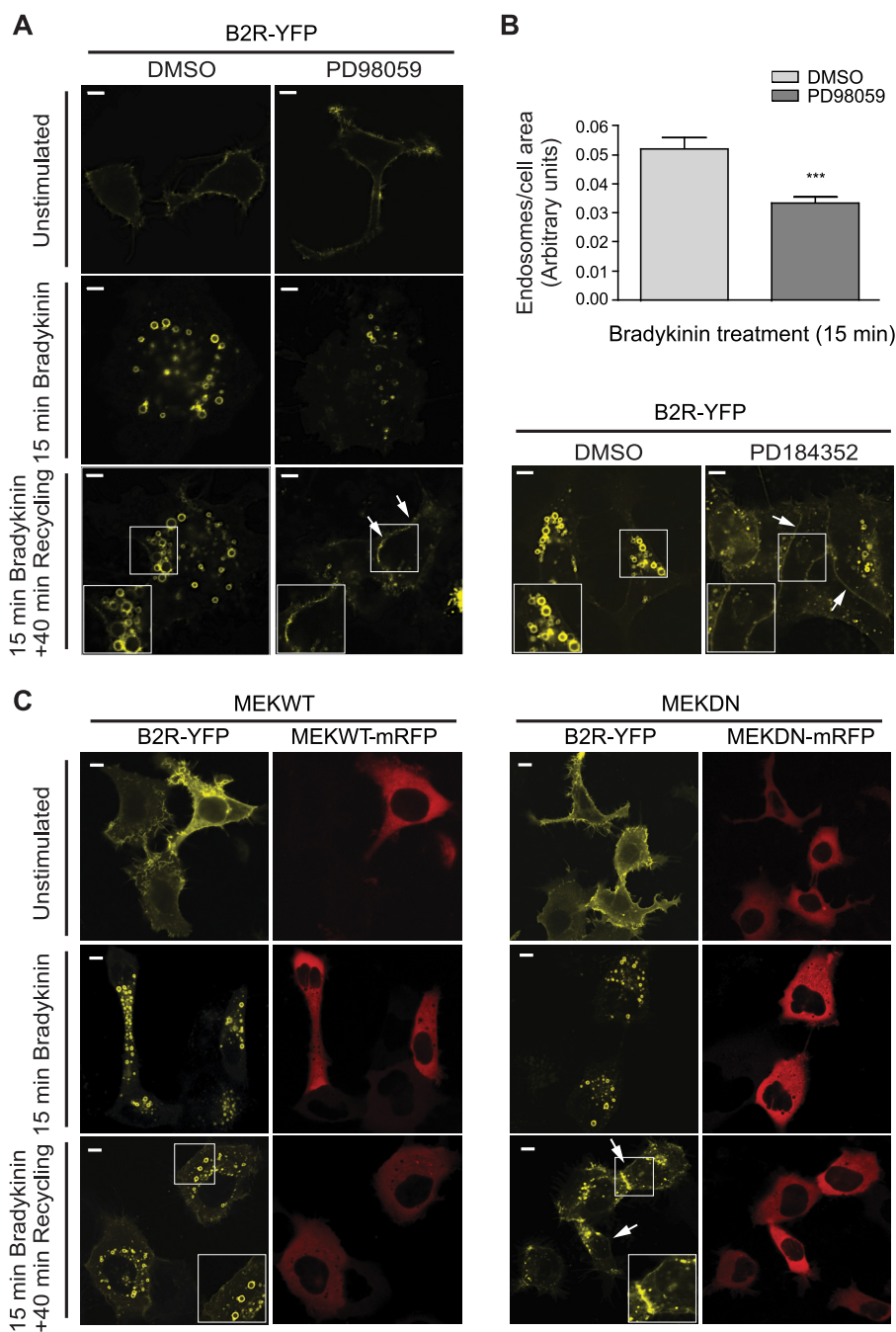


**FIGURE 4. Inhibition of MAPK alters B2R trafficking.** *A*, shown are representative confocal images of B2R-YFP internalization and receptor recycling in HEK293 cells. Cells expressing B2R-YFP and  $\beta$ -arrestin-2-myc were pretreated with either DMSO, PD98059 (20  $\mu$ M, 30 min; *bottom left panel*) or PD184352 (20  $\mu$ M, 30 min; *bottom right panel*), before being stimulated for 15 min with bradykinin (1  $\mu$ M) and imaged (*middle panels*), or washed to remove surface bound ligand and kept at 37 °C to allow receptor recycling for 40 min (*bottom panels*). *White arrows* depict receptor recycling at the plasma membrane. Enlargement of B2R-YFP localization is shown in the *left bottom insets* of recycling conditions. Three independent experiments were performed collecting a total of 55–71 cells. *B*, quantification of endosomes (>1  $\mu$ m) after 15 min bradykinin stimulation. Results are from three independent experiments with the respective quantification of 80 and 96 cells for the different conditions, and are expressed as the number of endosomes over the cell surface area. Statistical significance was analyzed by Student's *t* test; \*\*\*, *p* < 0.001. *C*, HEK293 cells were transiently transfected with B2R-YFP and the  $\beta$ -arrestin-2-myc and either MEKWT-mRFP or MEKDN-mRFP and were treated as in *A*. Shown are representative confocal images of B2R-YFP (*yellow*) and MEK-mRFP (*red*) depicting receptors trafficking to endosomes (*middle panel*) and their recycling to the plasma membrane (*bottom panel*). Results are representative images of three independent experiments surveying a total of 15–24 cells. Scale bars are 10  $\mu$ m.

to that observed for the rat  $\beta$ -arrestin-2 (Fig. 2*E*). Similarly to the rat  $\beta$ -arrestin-2, endosomal recovery of human  $\beta$ -arrestin-2 K178T became sensitive to MAPK inhibition, because its half-time recovery significantly decreased by more than 50% upon PD98059 treatment (Fig. 9, *C* and *F*). On the other hand, endosomal half-time recovery of the rat  $\beta$ -arrestin-2 T178K was

similar to that observed for the wild-type human  $\beta$ -arrestin-2 (Fig. 9, *D* and *F*), and was insensitive to MAPK inhibition, because treatment of cells with PD98059 did not significantly change its recovery time.

We next assessed how increasing the avidity of the B2R/ $\beta$ -arrestin-2 complex impacted MAPK signaling itself. To this



## Endosomal Signaling Function of $\beta$ -Arrestin on GPCR Trafficking

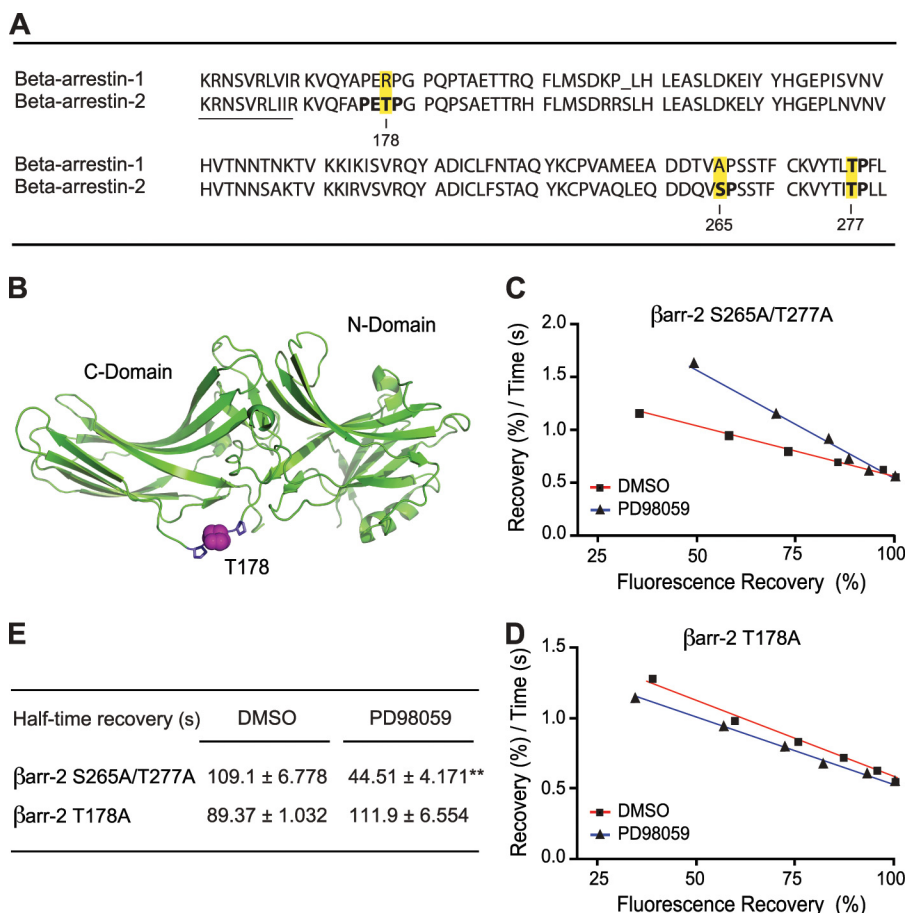


**FIGURE 5. Role of threonine 178 in B2R/ $\beta$ -arrestin-2 endosomal complex interaction.** *A*, amino acid sequence alignment is shown between  $\beta$ -arrestin-1 and  $\beta$ -arrestin-2. Potential MAPK motifs (S/TP) at position 178 (Thr), 265 (Ser), and 277 (Thr) in  $\beta$ -arrestin-2 are highlighted (*bold* and *yellow*) and the putative D-domain ERK1/2 docking site (KRNSVRLIIR) is underlined in  $\beta$ -arrestin-2 sequence. *B*, representation of the three-dimensional structure of the  $\beta$ -arrestin-2 using a cartoon visualization of the  $\alpha$ -helices and the  $\beta$ -sheets by PyMol software. The PET<sup>178</sup>P motif is presented by amino acid lines structure. *C* and *D*, FRAP analysis is presented as linear regression plots and was performed in HEK293 cells transiently transfected with HA-B2R and either the YFP-tagged  $\beta$ -arrestin-2 (*C*), S265A/T277A, or (*D*) T178A. Cells were either treated with DMSO or with PD98059 (20  $\mu$ M, 30 min), before being challenged with bradykinin (1  $\mu$ M, 15 min) as indicated in "Experimental Procedures." *E*, shown are half-time recovery (s) data of  $\beta$ -arrestin-2 S265A/T277A and  $\beta$ -arrestin-2 T178A mutants on B2R containing endosomes. Statistical analysis was performed by using Student's *t* test; \*\*, *p* < 0.01. Data are the mean  $\pm$  S.E. of three independent experiments, for 8–21 endosomes.

end we expressed either  $\beta$ -arrestin-2 T178D or  $\beta$ -arrestin-2 K178D in COS-7 cells, and assessed bradykinin-mediated ERK1/2 activation at different times. We used COS-7 cells, because they express low levels of endogenous  $\beta$ -arrestins and would allow better vetting mutant effects (31). In cells expressing either wild-type rat (Fig. 10, *A* and *B*) or human (Fig. 10, *C* and *D*)  $\beta$ -arrestin-2, we observed a biphasic activation of MAPK following bradykinin stimulation with an initial high response phase at 5 min, which is believed to be dependent on G proteins, followed by a lower, but more sustained  $\beta$ -arrestin-dependent ERK activation phase, which lasted up to 60 min. Expression of either rat  $\beta$ -arrestin-2 T178D (Fig. 10, *A* and *B*) or human  $\beta$ -arrestin-2 K178D (Fig. 10, *C* and *D*), significantly amplified (at 30 and 60 min) the agonist-mediated long-term MAPK phase. This sustained ERK1/2 activation phase was dependent on B2R internalization, because the expression of a non-functional Dynamin (Dyn K44A), which blocks GPCR internalization, prevented this response (Fig. 10, *E* and *F*). These data suggest that the hinge domain of  $\beta$ -arrestin-2, which controls its high affinity binding to receptors, also plays

an important role in the regulation of the B2R trafficking and signaling.

## DISCUSSION

We provide evidence for a new role of the MAPK signaling axis in the dynamic regulation of endosomal GPCR/ $\beta$ -arrestin-2 complexes and receptor trafficking. We identified a putative ERK1/2 phosphorylation site, which was present in the hinge domain of murine  $\beta$ -arrestin-2, but not  $\beta$ -arrestin-1. Moreover, the findings that the ERK regulatory site is present only in the murine  $\beta$ -arrestin-2 species (Fig. 9A) not only underscores the differences that exist in the endocytic functions between the two non-visual arrestin subtypes, but also suggest evolutionary divergences in the roles of  $\beta$ -arrestin-2. The identification of a key residue in the hinge domain of  $\beta$ -arrestin-2 (Thr<sup>178</sup>) also emphasizes the importance of this domain for regulating its interaction with GPCRs, which could be targeted to study the physiological roles of endosomal GPCR/ $\beta$ -arrestin-2 complexes. Based on our results, we propose a model where the formation of a receptor/ $\beta$ -arrestin/

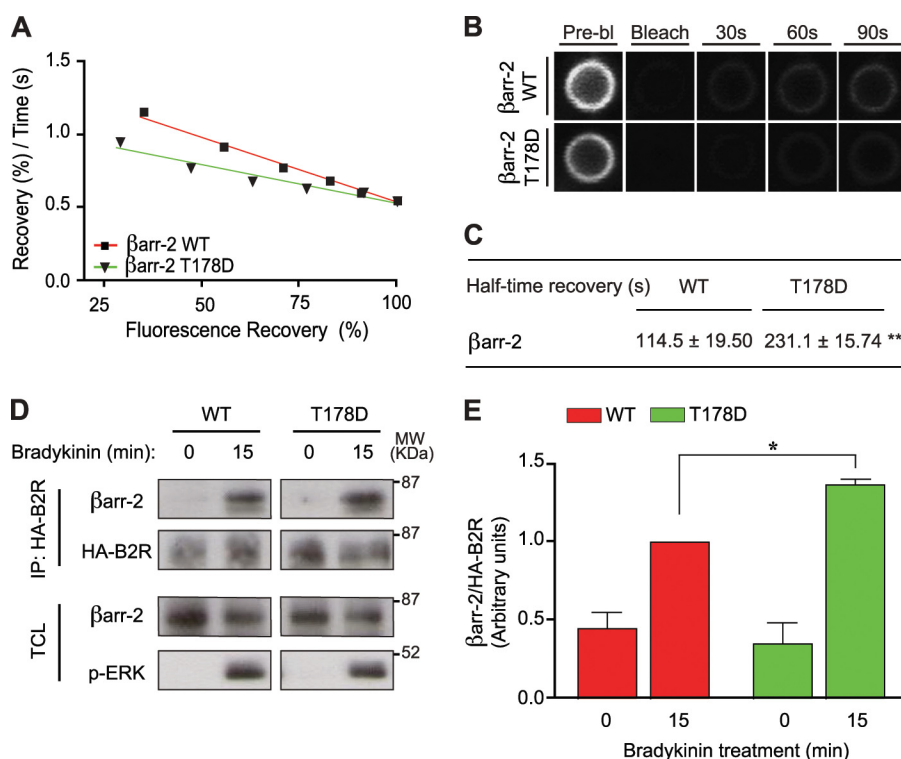


**FIGURE 6. Aspartic acid substitution at position 178 of  $\beta$ -arrestin-2 promote B2R/ $\beta$ -arrestin-2 endosomal complex formation.** *A*, shown are regression plots from FRAP experiments performed on HEK293 cells transiently transfected with HA-B2R and either  $\beta$ -arrestin-2 WT ( $\beta$ -arr-2 WT) or  $\beta$ -arrestin-2 T<sup>178</sup>D ( $\beta$ -arr-2 T178D) after 15 min of bradykinin stimulation (1  $\mu$ M) as described in "Experimental Procedures." *B*, representative confocal images from FRAP experiments of agonist stimulated cells expressing HA-B2R and either  $\beta$ -arr-2 WT or  $\beta$ -arr-2 T178D. Images are enlarged endosomes selected from 4–5 independent experiments assessing a total of 17 cells. *C*, shown are half-time recovery (s) data of  $\beta$ -arrestin-2 ( $\beta$ -arr-2) WT and T178D mutant on B2R containing endosomes, calculated from the linear regression analysis presented in *A*. Statistical analysis were performed by using Student's *t* test; \*\*,  $p < 0.01$ . Data are the mean  $\pm$  S.E. of at least three independent experiments, for 17 endosomes. *D*, HA-B2R stable cells expressing either  $\beta$ -arr-2 WT or T178D mutant were left unstimulated or challenged with bradykinin (1  $\mu$ M) for 15 min. Lysates from immuno-precipitated (IP) B2R were analyzed by Western blot using anti-HA (12CA5) and BARR3978 antibodies for receptor and  $\beta$ -arrestin-2 detection, respectively. Total cell lysates (TCL) were blotted for  $\beta$ -arrestin-2 and p-ERK. Shown are representative blots of three independent experiments. Molecular markers of 52 and 87 kDa are presented. *E*, densitometry analysis of immunoprecipitation experiments. Data represent the relative expression of  $\beta$ -arrestin-2 normalized to the amounts of B2R, as compared with the 15 min bradykinin stimulation, which is set at a 100% of the  $\beta$ -arr-2 WT condition. Densitometry results are presented as the mean  $\pm$  S.E. Statistical significance was analyzed by a two-way ANOVA followed by a Bonferroni post-test. \*,  $p < 0.05$ .

MAPK signaling complex plays an endosomal positive feedback role in the regulation of GPCRs trafficking and intracellular signaling (Fig. 11).

$\beta$ -Arrestins are implicated in both the trafficking and signaling of GPCRs (4, 5, 9). Here we have linked these two functions by providing evidence that signaling resulting from the scaffolding of MAPK with B2R/ $\beta$ -arrestin complexes controls the intracellular trafficking of receptors through a critical threonine residue in the hinge domain of  $\beta$ -arrestin-2. The role of MAPK in such regulatory mechanism is compelling for numerous reasons. First, we previously showed that following agonist stimulation of receptors, active ERK1/2 kinases are found in B2R/ $\beta$ -arrestin-2 complexes (20). Second, inhibiting ERK activity, using either pharmacological inhibitors (PD98059 or PD184352) of the upstream kinase MEK or expressing a dominant negative form of MEK-1, decreases the stability of B2R/ $\beta$ -arrestin-2 complexes in endosomes, and favors the faster recycling of receptor to the plasma membrane. Third, and consistent with its phosphorylation by MAPK, the hinge domain of  $\beta$ -arrestin-2 contains an ERK1/2 phosphorylation motif (PET<sup>178</sup>P) (32, 33), as well as possesses a putative D-domain ERK1/2 docking site (K/R<sub>2-3</sub>-X<sub>1-6</sub>-L/I-X-L/I) (e.g. positions 161–169: KR-NSVR-L-I-I) (Fig. 5) (34). Fourth, we gener-

ate a gain-of-function mutant for the human  $\beta$ -arrestin-2, which possesses a Lys residue instead of the Thr<sup>178</sup>. Substituting the Lys for a Thr residue in  $\beta$ -arrestin-2 rendered the receptor/ $\beta$ -arrestin-2 complex sensitive to MAPK inhibition, contrarily to its wild-type counterpart that remained insensitive. Fifth, we found that the substitution of Thr<sup>178</sup> for a negatively charged residue both in the human and rat  $\beta$ -arrestin-2, which would mimic a phosphorylated state, had opposite effects on the B2R/ $\beta$ -arrestin-2 complex stability and receptor trafficking compared with what was observed when inhibiting MAPK. Indeed, in such condition, we observed an increase in the endosomal lifetime of the B2R/ $\beta$ -arrestin-2 complex, and a decrease in receptor recycling to the plasma membrane.

Interestingly,  $\beta$ -arrestin-1 lacks such ERK "phosphorylatable" motif in its hinge domain, but is nonetheless regulated by ERK1/2 phosphorylation for its endocytic function. In clathrin-coated vesicles at the plasma membrane, ERK1/2 phosphorylates  $\beta$ -arrestin-1 at Ser<sup>412</sup> (absent in  $\beta$ -arrestin-2), with the consequence of regulating the binding to components of the clathrin coat (18). Our results suggest, however, that Ser<sup>412</sup> is not a target for the regulation of  $\beta$ -arrestin-1 interaction with B2R in the endosomes, because inhibiting MAPK did not affect the dynamics of such complex formation. MAPK phosphory-

## Endosomal Signaling Function of $\beta$ -Arrestin on GPCR Trafficking

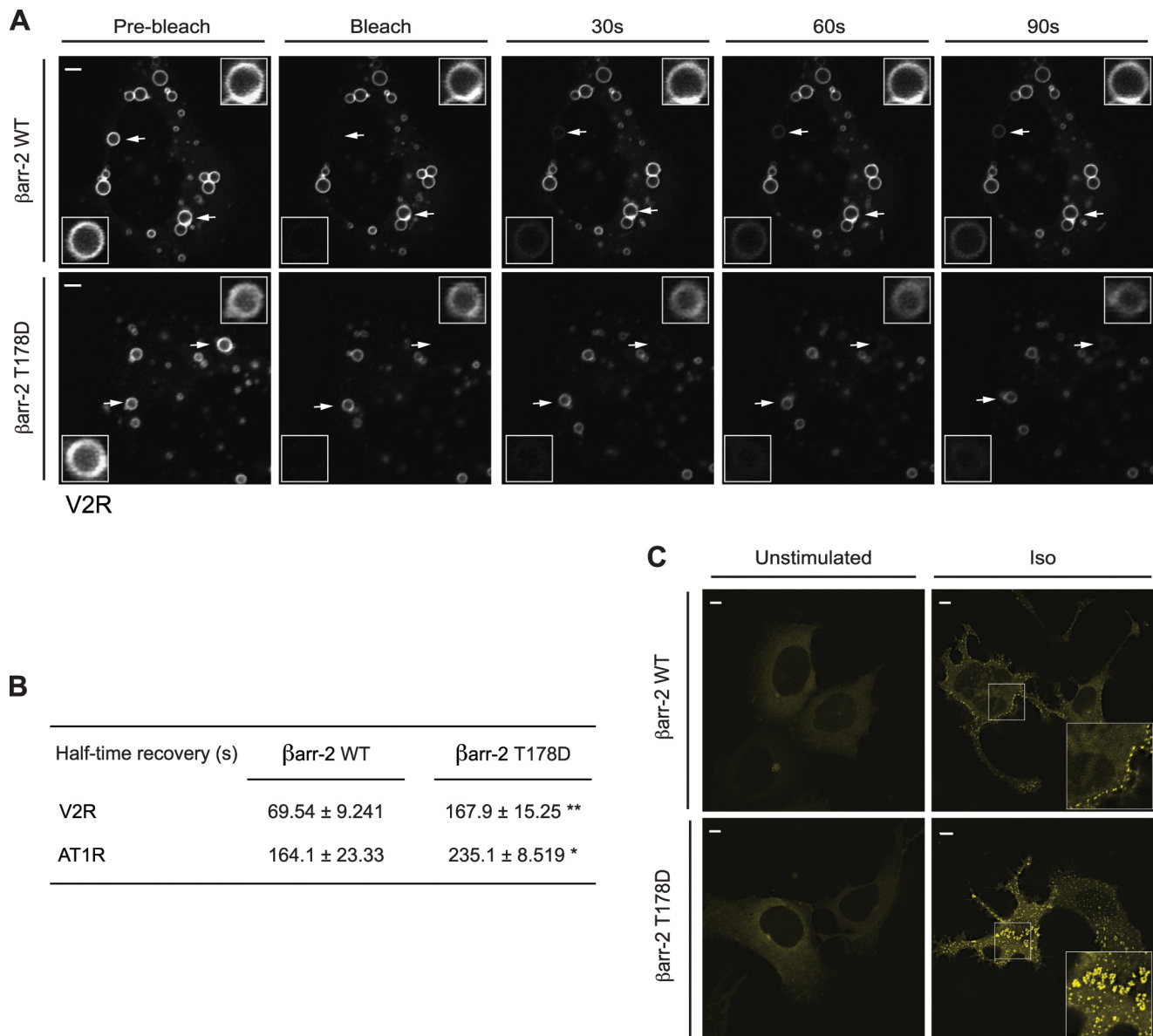


**FIGURE 7. The introduction of a negative charge at position 178 of  $\beta$ -arrestin-2 stabilizes its interaction with V2R, AT1R, and  $\beta$ 2AR.** *A*, representative images of FRAP experiments on endosomes from HEK293 cells expressing HA-V2R and either YFP-tagged  $\beta$ -arrestin-2 ( $\beta$ arr-2) WT or  $\beta$ arr-2 T178D mutant. Cells were treated with vasopressin (1  $\mu$ M) for 15 min and FRAP analysis was performed as in Fig. 1. Endosomes containing receptors and  $\beta$ -arrestins were selected (white arrows), and either bleached (bottom insets) or left unbleached (top insets). *B*, shown are half-time recovery (s) data of  $\beta$ -arrestin-2 ( $\beta$ arr-2) WT and T178D mutant endosomes from either HA-V2R or HA-AT1R-transfected cells. Statistical analysis was performed by using Student's *t* test; \*,  $p < 0.05$ , \*\*,  $p < 0.01$ . Data are the mean  $\pm$  S.E. of three independent experiments, for 11–17 endosomes. *C*, representative confocal images of HEK293 cells expressing the  $\beta$ 2AR with either YFP-tagged  $\beta$ arr-2 WT or  $\beta$ arr-2 T178D mutant, either stimulated with isoproterenol (1  $\mu$ M, right panels) for 15 min, or left unchallenged (left panels). An enlargement of the  $\beta$ -arrestin-2-YFP localization is shown in the bottom right insets of agonist-stimulated conditions. Scale bars are 10  $\mu$ m.

lation of  $\beta$ -arrestins has thus been conserved as a mechanism for controlling GPCR internalization and receptor trafficking, but seems to have diversified in terms of its spatio-temporal roles (e.g. plasma membrane versus endosomes).

How mechanistically the phosphorylation of, and/or the introduction of a negatively charged residue at position 178 in the hinge domain of  $\beta$ -arrestin-2 leads to increased affinity with activated receptors, is still unclear. However, crystallography studies and mutational analysis of different arrestins, which have provided some clues about the mechanics of GPCR/ $\beta$ -arrestin binding, may also hint to how the hinge domain and its phosphorylation regulate such interaction (35, 36). The binding of arrestins with activated, phosphorylated receptors follows a

multistep conformational rearrangement process. At basal states, the N- and C-domains of  $\beta$ -arrestins (Fig. 5B), which form two  $\beta$ -sandwich folds that contain the receptor-binding elements in their concave polybasic surface, are maintained distant to each other in a “locked” and elongated arrangement by two key intra-molecular interactions. A first interaction forms a network of electrostatic interacting residues in the interdomain interface defined as the polar core. The second key interaction involves the three-element arrangement of the N-domain (e.g. two  $\beta$ -strands, and one  $\alpha$ -helix) interacting with the C-tail of  $\beta$ -arrestins, which maintains the tail hidden in the core. Upon receptor activation, the engagement of the phosphorylated C-tail of GPCRs into arrestin neutralizes the positive charge of

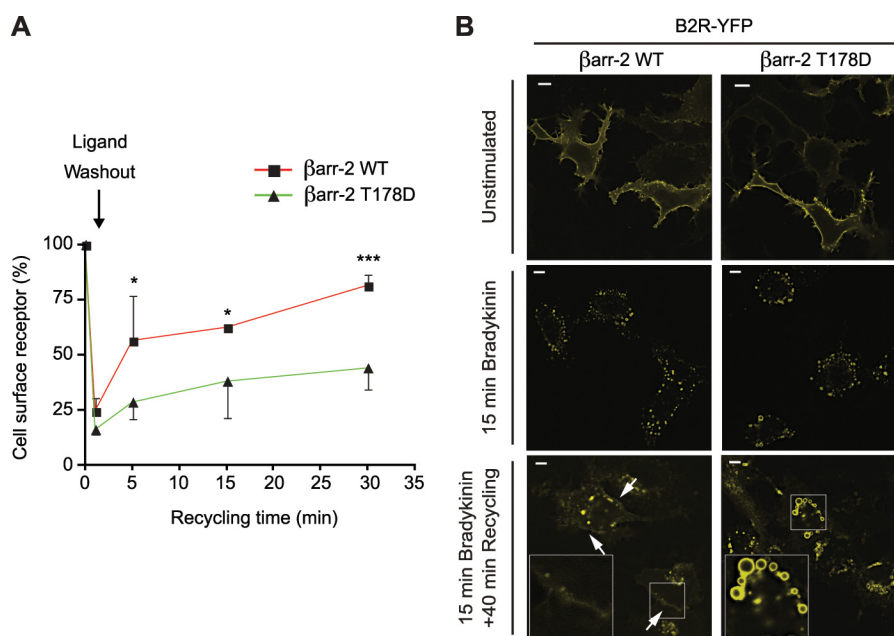


**FIGURE 8. Introducing a negative charge at position 178 of  $\beta$ -arrestin-2 impedes B2R recycling.** *A*, receptor recycling was assessed in COS-7 cells expressing the HA-B2R and either  $\beta$ -arrestin-2 ( $\beta$ -arr-2) WT or  $\beta$ -arr-2 T178D mutant as described in "Experimental Procedures." Data are the mean  $\pm$  S.E. of three independent experiments. Statistical significance was analyzed by a two-way ANOVA followed by a Bonferroni post-test was performed. \*,  $p < 0.05$ , \*\*\*,  $p < 0.001$ . *B*, representative confocal images of B2R internalization (*middle panels*), and recycling (*bottom panels*) in HEK293 cells as assessed in Fig. 4. *White arrows* depict receptor recycling at the plasma membrane and the enlargement of B2R-YFP localization is shown in the *left bottom insets* of recycling conditions. Scale bars are 10  $\mu$ m.

a key Arginine residue in the core domain (Arg<sup>175</sup> in arrestin and Arg<sup>170</sup> in  $\beta$ -arrestin-2). This will destabilize the polar core and the 3-element interactions and release arrestin C-tail, which in turn will result in closing the N- and C-domains onto the receptor in a "clam-like" movement (37). The hinge domain that links the N- and C-domains thus would maintain this closed state of arrestin, presumably through a new molecular rearrangement, which would stabilize furthermore the receptor/arrestin interaction. Introducing a negative charge at position 178 through phosphorylation could thus exert new electrostatic interactions of the hinge with other domains of  $\beta$ -arrestin-2 constraining it to maintain the closed arrangement of N- and C-domains on activated receptors, hence preserving a high affinity state of the receptor/ $\beta$ -arrestin complex (Fig. 11). Alternatively, but not necessarily mutually exclusive to the latter scenario, phosphorylation of Thr<sup>178</sup> and/or the introduction of a negative charge at this position, could facilitate the destabilization of the network interactions with Arg<sup>170</sup> in the core domain, allowing the more efficient "clam-like" closing of the N- and C-domains onto receptors. One would thus expect that under these conditions,  $\beta$ -arrestin-2 binds agonist-occupied receptors with higher affinity, and that at basal state if  $\beta$ -arrestin is prone to be phosphorylated in its hinge domain, receptors would also interact more efficiently with this "conformationally-primed"  $\beta$ -arrestin. Indeed, using the  $\beta$ -arrestin-2 T178D mutant, we converted a class A trafficking behavior to a class B one, such as in the case of the  $\beta$ 2AR, and increased the affinity of the receptor/ $\beta$ -arrestin-2 complex in the endosome with class B GPCR, such as with the V2R and the AT1R. However, we did not detect the constitutive internalization and/or complex formation in endosomes of  $\beta$ -arrestin-2 T178D with receptors. On the other hand, we did observe some ligand inde-

pendent internalization of B2R and endosomal complex formation between receptors and  $\beta$ -arrestin-2 in conditions overexpressing a constitutively active form of MEK1.<sup>4</sup> This suggests that  $\beta$ -arrestin-2 is preferentially targeted for phosphorylation when complexed with agonist-occupied receptors and that MAPK may also play other functions in the process of receptor internalization and trafficking, than only increasing the affinity of  $\beta$ -arrestin for the receptor. Although more work is needed to fully understand the role of MAPK on the structural rearrangement of  $\beta$ -arrestin-2, our findings strongly support the importance of the hinge domain in the regulation of  $\beta$ -arrestin binding to GPCRs.

Our findings are also coherent with other studies showing that long-lived endosomal GPCR/ $\beta$ -arrestin complexes facilitate continued intracellular MAPK signaling and affect receptor recycling at the plasma membrane (11, 38). We found a direct correlation between the increased affinity of B2R/ $\beta$ -arrestin-2 complexes in endosomes and the sustained MAPK signaling, as well as with the reduced kinetics of receptor recycling from endosomes back to the plasma membrane.

Our data not only highlight differences in the regulation of receptor/ $\beta$ -arrestin complexes, but also imply that differences exist in the intrinsic affinity between  $\beta$ -arrestin-1 and  $\beta$ -arrestin-2, as well as among  $\beta$ -arrestin-2 from different species. For instance, the rat  $\beta$ -arrestin-2 had a greater affinity for B2R than the rat  $\beta$ -arrestin-1 and formed a tighter complex with B2R than human  $\beta$ -arrestin-2. These findings suggest that other determinants in each  $\beta$ -arrestins must also be involved in stabilizing the interaction with receptors. Other regulatory mech-

<sup>4</sup> E. Khoury and S.A. Laporte, unpublished observations.

## Endosomal Signaling Function of $\beta$ -Arrestin on GPCR Trafficking

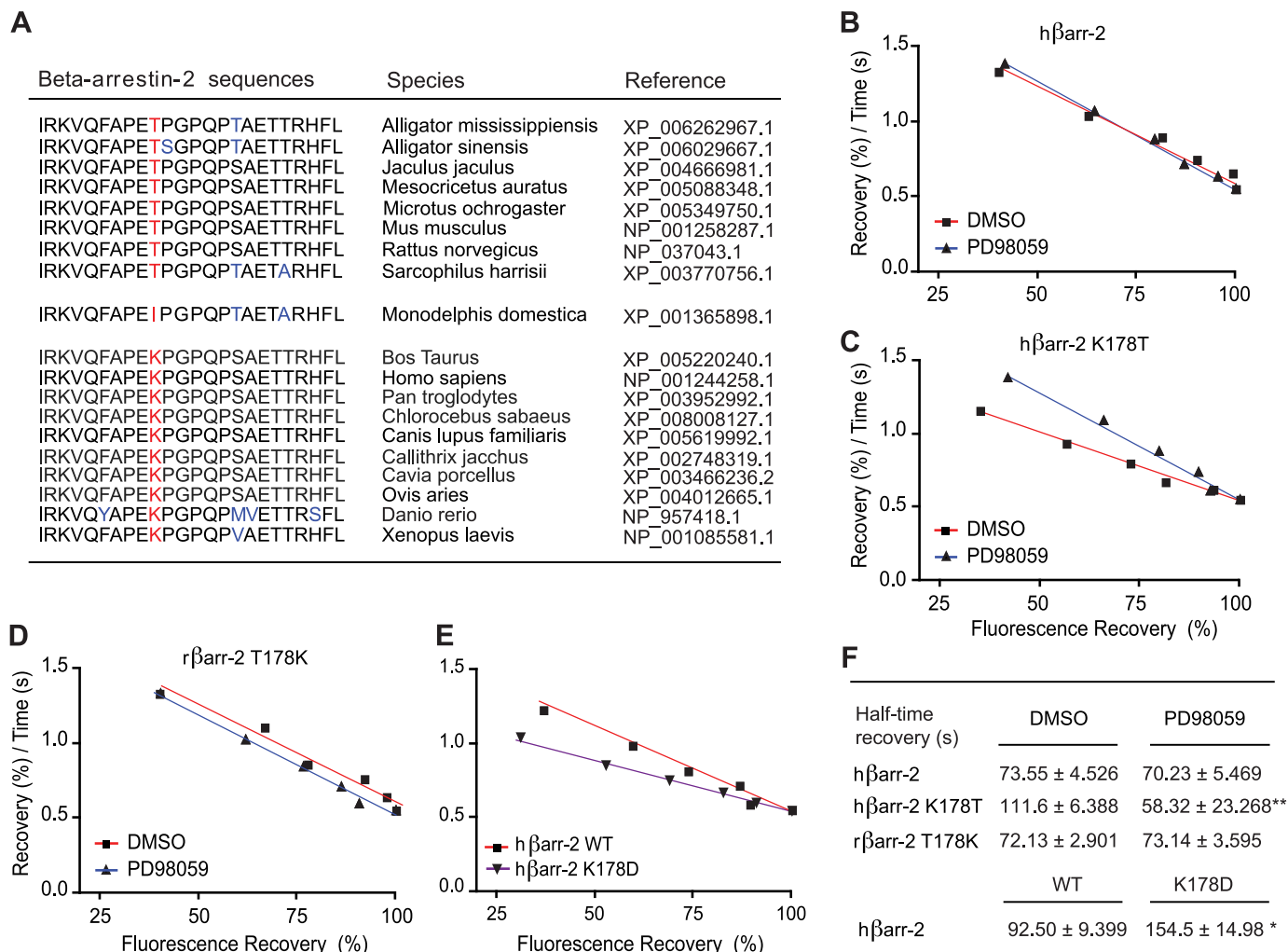


**FIGURE 9. Position 178 in  $\beta$ -arrestin-2 regulates the interaction between B2R and arrestins in endosomes.** A, interspecies alignment of the hinge domain of  $\beta$ -arrestin-2 sequences. Using BLAST (bl2seq), amino acid sequences were grouped by different PEXP conserved motif. Red letters indicate the identified MAPK motif (PETP), which is converted to a lysine or an isoleucine among species, and blue letters show the non-conserved amino acids. Other than homo sapiens, Lys<sup>178</sup> is also conserved among different species such as, *Camelus ferus* (EPY84367.1), *Ceratotherium simum simum* (XP\_004433246.1), *Chinchilla lanigera* (XP\_005399652.1), *Ailuropoda melanoleuca* (XP\_002924519.1), *Tupaia chinensis* (XP\_006151916.1), *Pan paniscus* (XP\_003810257.1), *Sus scrofa* (ACF37110.1), *Trichechus manatus latirostris* (XP\_004376131.1), *Otolemur garnettii* (XP\_003791244.1), *Papio Anubis* (XP\_003912182), *Saimiri boliviensis boliviensis* (XP\_003931443.1), *Orcinus orca* (XP\_004267017.1), *Dasyypus novemcinctus* (XP\_004475312.1), *Sorex araneus* (XP\_004604974.1), *Octodon degus* (XP\_004638414.1), *Mustela putorius furo* (XP\_004760457.1), *Heterocephalus glaber* (XP\_004901403.1), *Pantholops hodgsonii* (XP\_005967979.1), *Vicugna pacos* (XP\_006217626.1), *Nomascus leucogenys* (XP\_004091595.1), *Odobenus rosmarus divergens* (XP\_004398622.1), *Ochotona princeps* (XP\_004594896.1), *Ictidomys tridecemlineatus* (XP\_005337434.1), *Myotis lucifugus* (XP\_006102837.1). B, C, D, and E, FRAP analysis is presented as regression plots and was performed in HEK293 cells transiently transfected with HA-B2R and either the YFP-tagged (B) human  $\beta$ -arrestin-2 (h $\beta$ arr-2), (C) h $\beta$ arr-2 K178T, (D) rat  $\beta$ -arrestin-2 (r $\beta$ arr-2) T178K, or (E) h $\beta$ arr-2 K178D after 15 min of bradykinin stimulation (1  $\mu$ M), and either DMSO or PD98059 (20  $\mu$ M, 30 min) treatments as described in Fig. 1 and in "Experimental Procedures." F, shown are half-time recovery (s) of YFP-tagged h $\beta$ arr-2 and r $\beta$ arr-2 mutants, calculated from the linear regression analysis presented in panels B, C, D, and E. Statistical analysis was performed by using Student's t test; \*,  $p < 0.05$ ; \*\*,  $p < 0.01$ . Data are the mean  $\pm$  S.E. of at least three independent experiments for 14–24 endosomes.

anisms than MAPK phosphorylation have also been implicated in regulating the affinity of  $\beta$ -arrestins with GPCRs. For example,  $\beta$ -arrestin-2 undergoes ubiquitination on two lysines residues (Lys<sup>11</sup> and Lys<sup>12</sup>), which stabilizes its interaction with different receptors (39). Although we did not specifically assess whether Lys<sup>178</sup> in the human  $\beta$ -arrestin-2 was a target for ubiquitination, we do not believe that such mode of regulation is at play here, because we did not observe changes in the lifetime of endosomal B2R/ $\beta$ -arrestins complexes when the lysine was substituted for an alanine (K178A).<sup>4</sup> From our data, we can draw an affinity hierarchy order for  $\beta$ -arrestin interaction with receptors: rat  $\beta$ -arrestin-2 T178D > human  $\beta$ -arrestin-2 K178D > rat  $\beta$ -arrestin-2  $\approx$  human  $\beta$ -arrestin-2 K178T > rat

$\beta$ -arrestin-2 T178K  $\approx$  human  $\beta$ -arrestin-2 > rat  $\beta$ -arrestin-1. We also propose that such characteristics could be used to study the role of receptor/ $\beta$ -arrestin complexes in signaling and trafficking of GPCRs. However, an important aspect to consider when performing such studies in cells is the species and/or levels of endogenous  $\beta$ -arrestins present, as it is the case for example between HEK293 (e.g. human  $\beta$ -arrestin) and COS-7 cells (e.g. African green monkey, *Chlorocebus sabaeus*, Fig. 9A) because they may differentially compete and affect the responses mediated by a tagged  $\beta$ -arrestin exogenously expressed.

The hinge domain of  $\beta$ -arrestins is an exposed and molecularly flexible structure (37, 40), which mechanistically provides

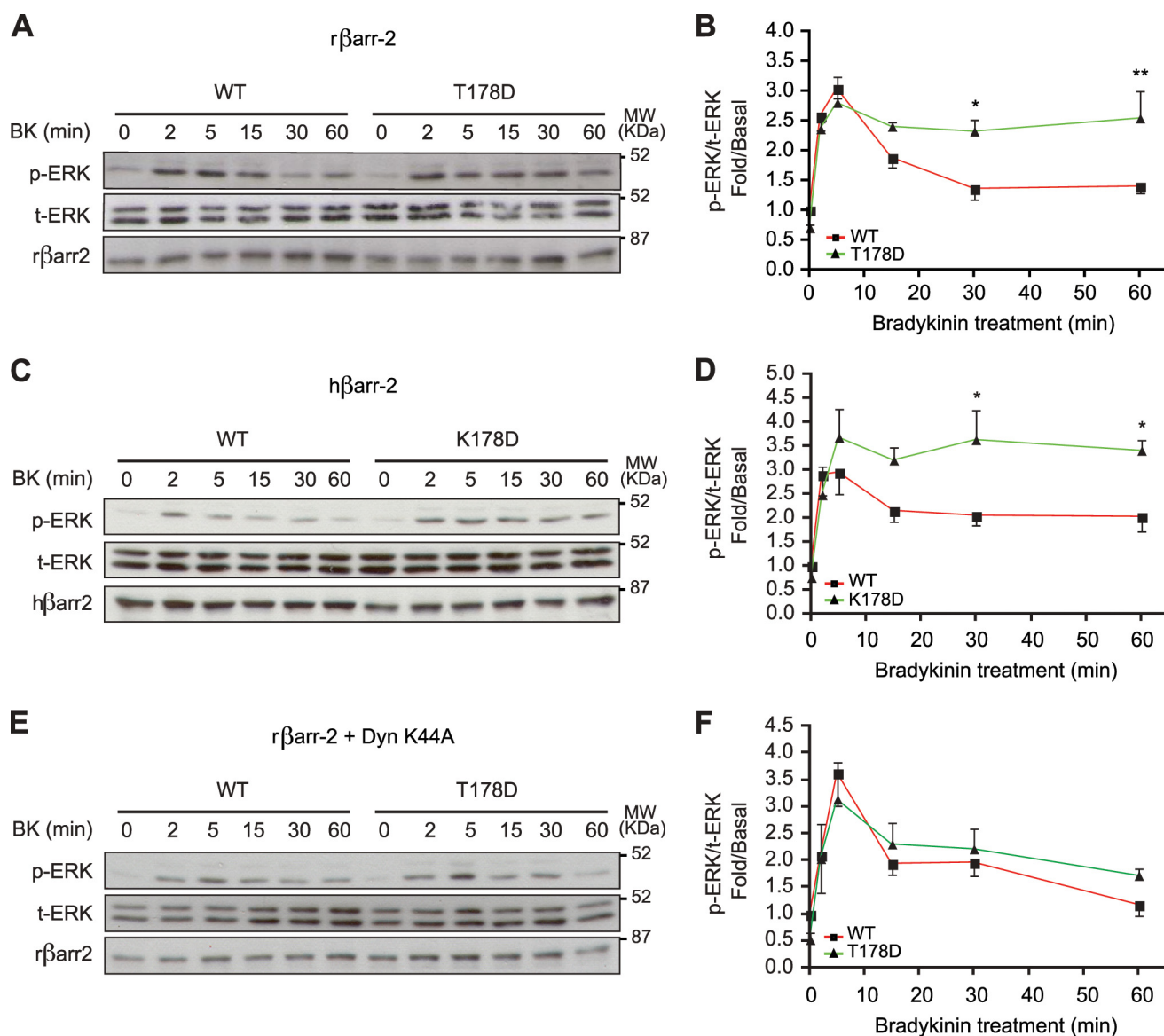


FIGURE 10. Aspartic acid substitution at position 178 of  $\beta$ -arrestin-2 promotes sustained B2R-dependent MAPK activation. *A*, *C*, and *E*, shown are representative immunoblots of ERK activation from COS-7 cells expressing HA-B2R and either (A) rat  $\beta$ -arrestin-2 ( $r\beta$ arr-2) WT or  $r\beta$ arr-2 T178D mutant, and (C) either human  $\beta$ -arrestin-2 ( $h\beta$ arr-2) WT or  $h\beta$ arr-2 K178D mutant, and challenged with bradykinin (1  $\mu$ M) for the indicated time. *E*, cells were transfected as in *A* with the addition of Dynamin K44A (Dyn K44A). Lysates were immunoblotted for phosphorylated ERK (p-ERK), total ERK (t-ERK) and  $\beta$ -arrestin-2 (BARR3978). Molecular markers of 52 and 87 kDa are depicted. *B*, *D*, and *F*, densitometry analysis of data from *A*, *C*, and *E*, respectively, which represents the mean  $\pm$  S.E. of minimum three independent experiments. p-ERK signals were normalized to that of t-ERK, and compared with non-treated cells for statistical analysis using a two-way ANOVA followed test followed by a Bonferroni post-test. \*,  $p < 0.05$ ; \*\*,  $p < 0.01$ .

an ideal localization for a phosphorylation regulatory site such as the one for MAPK. However, this motif is not found in all  $\beta$ -arrestin-2 species (Fig. 9A), and seems to have evolved differently among them. Indeed, the “phosphorylatable” threonine of the PXTTP motif is present both in mice and rat, but not all rodents, and in most other animals, a Lysine residue replaces it. Interestingly, the threonine residue is also found in more distantly related animals (see, Fig. 9). Because the process of phosphorylation of proteins would require energy, this suggests that contrarily to other mammals, the rat and mice have preserved this ancestral mode of regulation (e.g. the increased endosomal  $\beta$ -arrestin-2 interaction with GPCR upon the hinge phosphorylation). In our limited phylogenetic analysis, we did not identify gain-of-function mutations (e.g. substitutions of Thr<sup>178</sup> for

either Asp or Glu). This, however, was less surprising since non-synonymous mutations would require the spontaneous mutation of at least two nucleotides for converting a threonine (or a lysine) into either an Aspartic or Glutamic acids, contrarily to only one for generating a threonine from a lysine (e.g. ACA  $\rightarrow$  AAA, respectively), as it is the case here for the difference between the rat and the human  $\beta$ -arrestin-2. Moreover, the location of this regulatory site in rat  $\beta$ -arrestin-2 must also be critical, because its position did not change, as it often occurs in evolutionary processes between species for post-translational modified sites (e.g. phosphosites or ubiquitination ones) contained in disordered and/or flexible regions of proteins (41).

Our findings also open questions about the species-specific  $\beta$ -arrestin-dependent MAPK regulation of receptor trafficking

## Endosomal Signaling Function of $\beta$ -Arrestin on GPCR Trafficking

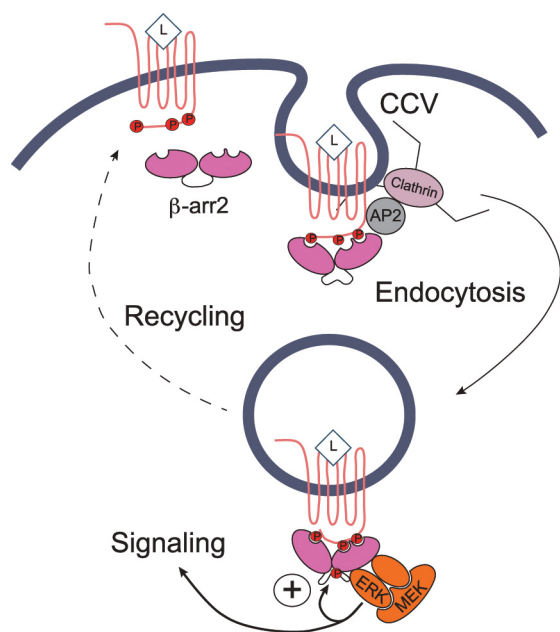


**FIGURE 11. Positive feedback mechanism regulation of B2R trafficking and intracellular MAPK signaling by the scaffolding function of  $\beta$ -arrestin-2.** Ligand binding to B2R promotes G protein-kinase-dependent receptor phosphorylation, the binding of  $\beta$ -arrestin-2 ( $\beta$ -arr2) to receptors and the clathrin-dependent internalization of the complex into endosomes. The B2R/ $\beta$ -arrestin-2 then recruits a MAPK complex composed of MEK, ERK1/2 and presumably Raf (not shown) for intracellular signaling. The introduction of a negative charge in the hinge domain of  $\beta$ -arrestin-2, such as in the case of the phosphorylation of Thr<sup>178</sup> by MAPK, increases furthermore the avidity of the B2R/ $\beta$ -arrestin-2 complex, allowing continued ERK1/2 signaling in the endosome, which further maintains, through a positive feedback mechanism, the high affinity binding state of the complex, leading to slower recycling of the receptor to the plasma membrane. CCV, clathrin-coated vesicles; AP2, clathrin adaptor protein 2.

and signaling on the physiological outcomes. Although the reasons remain unclear, regulating the interaction between GPCRs and  $\beta$ -arrestin-2 in endosomes, hence controlling some aspects of receptor signaling, e.g. at the plasma membrane by preventing receptor recycling and/or favoring the signaling inside the cell, might play differential physiological functions in rodent *versus* human. New evidence suggests that the GPCR/ $\beta$ -arrestin signaling axis may also be an important therapeutic target. Indeed, recent findings have shown that a biased ligand of AT1R favoring the GPCR/ $\beta$ -arrestin-2 signaling complex is cardio-protective in rodents (42–44). The extent to which Thr<sup>178</sup> phosphorylation of  $\beta$ -arrestin-2 and the sustained endosomal AT1R/ $\beta$ -arrestin signaling to MAPKs contribute to these effects are however still unclear. On the other hand, if such mechanisms is involved, it would only presumably contribute partially to this effect, because similar cardio-protective roles of the AT1R-biased ligand have also been reported in dogs, whose  $\beta$ -arrestin-2, like in human, share a Lys residue at this position (Fig. 9) (45). Notwithstanding this latter possibility, the existence of differential MAPK-dependent regulation of receptor/ $\beta$ -arrestin signaling complexes for GPCRs should be considered when studying their physiological and pathophysiological roles in different animal models, as it may provide a therapeutic rationale for targeting such endosomal signaling complexes.

In summary, we provide here the first direct evidence for a role of MAPK in the endosomal trafficking of GPCRs. We iden-

tified a new regulatory site in the hinge domain of  $\beta$ -arrestin-2, which diverged among different species, and when targeted by phosphorylation not only increases the lifetime of receptor/ $\beta$ -arrestin complex in endosomes, but also the intracellular signaling and trafficking of receptors. Taking advantage of this “regulatable” property of  $\beta$ -arrestin-2 should further our understanding of the role of the GPCR/ $\beta$ -arrestin signaling axis in endosomes.

*Acknowledgments*—We thank Drs. M. Bouvier, C. Le Gouill, and S. Armando, and all the members of the Laporte laboratory for helpful discussions, and Dr. C. Rocheleau for critical reading of the manuscript.

## REFERENCES

1. Fredriksson, R., Lagerström, M. C., Lundin, L. G., and Schiöth, H. B. (2003) The G-protein-coupled receptors in the human genome form five main families. Phylogenetic analysis, paralogon groups, and fingerprints. *Mol. Pharmacol.* **63**, 1256–1272
2. Lagerström, M. C., and Schiöth, H. B. (2008) Structural diversity of G protein-coupled receptors and significance for drug discovery. *Nat. Rev. Drug Discov.* **7**, 339–357
3. Ma, P., and Zimmel, R. (2002) Value of novelty? *Nat. Rev. Drug Discov.* **1**, 571–572
4. Claing, A., Laporte, S. A., Caron, M. G., and Lefkowitz, R. J. (2002) Endocytosis of G protein-coupled receptors: roles of G protein-coupled receptor kinases and  $\beta$ -arrestin proteins. *Prog. Neurobiol.* **66**, 61–79
5. Lefkowitz, R. J., and Shenoy, S. K. (2005) Transduction of receptor signals by  $\beta$ -arrestins. *Science* **308**, 512–517
6. Gurevich, E. V., and Gurevich, V. V. (2006) Arrestins: ubiquitous regulators of cellular signaling pathways. *Genome Biol.* **7**, 236
7. Lefkowitz, R. J. (1998) G protein-coupled receptors. III. New roles for receptor kinases and  $\beta$ -arrestins in receptor signaling and desensitization. *J. Biol. Chem.* **273**, 18677–18680
8. Luttrell, L. M., and Lefkowitz, R. J. (2002) The role of  $\beta$ -arrestins in the termination and transduction of G-protein-coupled receptor signals. *J. Cell Sci.* **115**, 455–465
9. Moore, C. A., Milano, S. K., and Benovic, J. L. (2007) Regulation of receptor trafficking by GRKs and arrestins. *Annu. Rev. Physiol.* **69**, 451–482
10. Oakley, R. H., Laporte, S. A., Holt, J. A., Caron, M. G., and Barak, L. S. (2000) Differential affinities of visual arrestin,  $\beta$  arrestin1, and  $\beta$  arrestin2 for G protein-coupled receptors delineate two major classes of receptors. *J. Biol. Chem.* **275**, 17201–17210
11. Simaan, M., Bédard-Goulet, S., Fessart, D., Gratton, J. P., and Laporte, S. A. (2005) Dissociation of  $\beta$ -arrestin from internalized bradykinin B2 receptor is necessary for receptor recycling and resensitization. *Cell Signal* **17**, 1074–1083
12. DeFea, K. A., Zalevsky, J., Thoma, M. S., Déry, O., Mullins, R. D., and Bunnett, N. W. (2000)  $\beta$ -arrestin-dependent endocytosis of proteinase-activated receptor 2 is required for intracellular targeting of activated ERK1/2. *J. Cell Biol.* **148**, 1267–1281
13. Luttrell, L. M., Roudabush, F. L., Choy, E. W., Miller, W. E., Field, M. E., Pierce, K. L., and Lefkowitz, R. J. (2001) Activation and targeting of extracellular signal-regulated kinases by  $\beta$ -arrestin scaffolds. *Proc. Natl. Acad. Sci. U.S.A.* **98**, 2449–2454
14. Tohgo, A., Pierce, K. L., Choy, E. W., Lefkowitz, R. J., and Luttrell, L. M. (2002)  $\beta$ -Arrestin scaffolding of the ERK cascade enhances cytosolic ERK activity but inhibits ERK-mediated transcription following angiotensin AT1a receptor stimulation. *J. Biol. Chem.* **277**, 9429–9436
15. Fessart, D., Simaan, M., and Laporte, S. A. (2005) c-Src regulates clathrin adaptor protein 2 interaction with  $\beta$ -arrestin and the angiotensin II type 1 receptor during clathrin-mediated internalization. *Mol. Endocrinol.* **19**, 491–503
16. Fessart, D., Simaan, M., Zimmerman, B., Comeau, J., Hamdan, F. F., Wiseman, P. W., Bouvier, M., and Laporte, S. A. (2007) Src-dependent phos-

- phorylation of  $\beta$ 2-adaptin dissociates the  $\beta$ -arrestin-AP-2 complex. *J. Cell Sci.* **120**, 1723–1732
17. Lin, F. T., Krueger, K. M., Kendall, H. E., Daaka, Y., Fredericks, Z. L., Pitcher, J. A., and Lefkowitz, R. J. (1997) Clathrin-mediated endocytosis of the  $\beta$ -adrenergic receptor is regulated by phosphorylation/dephosphorylation of  $\beta$ -arrestin1. *J. Biol. Chem.* **272**, 31051–31057
  18. Lin, F. T., Miller, W. E., Luttrell, L. M., and Lefkowitz, R. J. (1999) Feedback regulation of  $\beta$ -arrestin1 function by extracellular signal-regulated kinases. *J. Biol. Chem.* **274**, 15971–15974
  19. Ahn, S., Maudsley, S., Luttrell, L. M., Lefkowitz, R. J., and Daaka, Y. (1999) Src-mediated tyrosine phosphorylation of dynamin is required for  $\beta$ 2-adrenergic receptor internalization and mitogen-activated protein kinase signaling. *J. Biol. Chem.* **274**, 1185–1188
  20. Zimmerman, B., Simaan, M., Akoume, M. Y., Houry, N., Chevallier, S., Séguéla, P., and Laporte, S. A. (2011) Role of  $\beta$ -arrestins in bradykinin B2 receptor-mediated signalling. *Cell Signal* **23**, 648–659
  21. Zimmerman, B., Simaan, M., Lee, M. H., Luttrell, L. M., and Laporte, S. A. (2009) c-Src-mediated phosphorylation of AP-2 reveals a general mechanism for receptors internalizing through the clathrin pathway. *Cell Signal* **21**, 103–110
  22. Laporte, S. A., Oakley, R. H., Zhang, J., Holt, J. A., Ferguson, S. S., Caron, M. G., and Barak, L. S. (1999) The  $\beta$ 2-adrenergic receptor/ $\beta$ -arrestin complex recruits the clathrin adaptor AP-2 during endocytosis. *Proc. Natl. Acad. Sci. U.S.A.* **96**, 3712–3717
  23. Zimmerman, B., Beautrait, A., Aguila, B., Charles, R., Escher, E., Claing, A., Bouvier, M., and Laporte, S. A. (2012) Differential  $\beta$ -arrestin-dependent conformational signaling and cellular responses revealed by angiotensin analogs. *Sci. Signal* **5**, ra33
  24. Zhang, J., Barak, L. S., Anborgh, P. H., Laporte, S. A., Caron, M. G., and Ferguson, S. S. (1999) Cellular trafficking of G protein-coupled receptor/ $\beta$ -arrestin endocytic complexes. *J. Biol. Chem.* **274**, 10999–11006
  25. Aguila, B., Simaan, M., and Laporte, S. A. (2011) Study of G protein-coupled receptor/ $\beta$ -arrestin interactions within endosomes using FRAP. *Methods Mol. Biol.* **756**, 371–380
  26. Gousseva, V., Simaan, M., Laporte, S. A., and Swain, P. S. (2008) Inferring the lifetime of endosomal protein complexes by fluorescence recovery after photobleaching. *Biophys. J.* **94**, 679–687
  27. Chen, Y. S., Huang, W. H., Hong, S. Y., Tsay, Y. G., and Chen, P. J. (2008) ERK1/2-mediated phosphorylation of small hepatitis delta antigen at serine 177 enhances hepatitis delta virus antigenomic RNA replication. *J. Virol.* **82**, 9345–9358
  28. Nagasaka, K., Pim, D., Massimi, P., Thomas, M., Tomaić, V., Subbaiah, V. K., Kranjec, C., Nakagawa, S., Yano, T., Taketani, Y., Myers, M., and Banks, L. (2010) The cell polarity regulator hScrib controls ERK activation through a KIM site-dependent interaction. *Oncogene* **29**, 5311–5321
  29. Oakley, R. H., Laporte, S. A., Holt, J. A., Barak, L. S., and Caron, M. G. (1999) Association of  $\beta$ -arrestin with G protein-coupled receptors during clathrin-mediated endocytosis dictates the profile of receptor resensitization. *J. Biol. Chem.* **274**, 32248–32257
  30. Oakley, R. H., Laporte, S. A., Holt, J. A., Barak, L. S., and Caron, M. G. (2001) Molecular determinants underlying the formation of stable intracellular G protein-coupled receptor- $\beta$ -arrestin complexes after receptor endocytosis. *J. Biol. Chem.* **276**, 19452–19460
  31. Ménard, L., Ferguson, S. S., Zhang, J., Lin, F. T., Lefkowitz, R. J., Caron, M. G., and Barak, L. S. (1997) Synergistic regulation of  $\beta$ 2-adrenergic receptor sequestration: intracellular complement of  $\beta$ -adrenergic receptor kinase and  $\beta$ -arrestin determine kinetics of internalization. *Mol. Pharmacol.* **51**, 800–808
  32. Pearson, R. B., and Kemp, B. E. (1991) Protein kinase phosphorylation site sequences and consensus specificity motifs: tabulations. *Methods Enzymol.* **200**, 62–81
  33. Songyang, Z., Lu, K. P., Kwon, Y. T., Tsai, L. H., Filhol, O., Cochet, C., Brickey, D. A., Soderling, T. R., Bartleson, C., Graves, D. J., DeMaggio, A. J., Hoekstra, M. F., Blenis, J., Hunter, T., and Cantley, L. C. (1996) A structural basis for substrate specificities of protein Ser/Thr kinases: primary sequence preference of casein kinases I and II, NIMA, phosphorylase kinase, calmodulin-dependent kinase II, CDK5, and Erk1. *Mol. Cell Biol.* **16**, 6486–6493
  34. Tanoue, T., and Nishida, E. (2003) Molecular recognitions in the MAP kinase cascades. *Cell Signal* **15**, 455–462
  35. Shukla, A. K., Manglik, A., Kruse, A. C., Xiao, K., Reis, R. I., Tseng, W. C., Staus, D. P., Hilger, D., Uysal, S., Huang, L. Y., Paduch, M., Tripathi-Shukla, P., Koide, A., Koide, S., Weis, W. I., Kossiakoff, A. A., Kobilka, B. K., and Lefkowitz, R. J. (2013) Structure of active  $\beta$ -arrestin-1 bound to a G-protein-coupled receptor phosphopeptide. *Nature* **497**, 137–141
  36. Vishnivetskiy, S. A., Hirsch, J. A., Velez, M. G., Gurevich, Y. V., and Gurevich, V. V. (2002) Transition of arrestin into the active receptor-binding state requires an extended interdomain hinge. *J. Biol. Chem.* **277**, 43961–43967
  37. Gurevich, V. V., and Benovic, J. L. (1997) Mechanism of phosphorylation-recognition by visual arrestin and the transition of arrestin into a high affinity binding state. *Mol. Pharmacol.* **51**, 161–169
  38. Tohgo, A., Choy, E. W., Gesty-Palmer, D., Pierce, K. L., Laporte, S., Oakley, R. H., Caron, M. G., Lefkowitz, R. J., and Luttrell, L. M. (2003) The stability of the G protein-coupled receptor- $\beta$ -arrestin interaction determines the mechanism and functional consequence of ERK activation. *J. Biol. Chem.* **278**, 6258–6267
  39. Shenoy, S. K., and Lefkowitz, R. J. (2005) Receptor-specific ubiquitination of  $\beta$ -arrestin directs assembly and targeting of seven-transmembrane receptor signalosomes. *J. Biol. Chem.* **280**, 15315–15324
  40. Gnad, F., Ren, S., Cox, J., Olsen, J. V., Macek, B., Oroshi, M., and Mann, M. (2007) PHOSIDA (phosphorylation site database): management, structural and evolutionary investigation, and prediction of phosphosites. *Genome Biol.* **8**, R250
  41. Hagai, T., Tóth-Petróczy, Á., Azia, A., and Levy, Y. (2012) The origins and evolution of ubiquitination sites. *Mol. Biosyst.* **8**, 1865–1877
  42. Violin, J. D., Soergel, D. G., DeWire, S. M., Yamashita, D., Rominger, D., Whalen, E. J., Gowen, M., and Lark, M. W. (2010) TRV120027, a  $\beta$ -Arrestin Biased Ligand at the Angiotensin II Type 1 Receptor, Produces Unique Pharmacology and Is a Novel Potential Therapy for Heart Failure. *J. Card. Fail.* **16**, S72–S72
  43. Violin, J. D., DeWire, S. M., Yamashita, D., Rominger, D. H., Nguyen, L., Schiller, K., Whalen, E. J., Gowen, M., and Lark, M. W. (2010) Selectively engaging  $\beta$ -arrestins at the angiotensin II type 1 receptor reduces blood pressure and increases cardiac performance. *J. Pharmacol. Exp. Therap.* **335**, 572–579
  44. Kim, K. S., Abraham, D., Williams, B., Violin, J. D., Mao, L., and Rockman, H. A. (2012)  $\beta$ -Arrestin-biased AT1R stimulation promotes cell survival during acute cardiac injury. *Am. J. Physiol.* **303**, H1001–H1010
  45. Boerrigter, G., Lark, M. W., Whalen, E. J., Soergel, D. G., Violin, J. D., and Burnett, J. C. (2011) Cardiorenal Actions of TRV120027, a Novel  $\beta$ -Arrestin-Biased Ligand at the Angiotensin II Type I Receptor, in Healthy and Heart Failure Canines A Novel Therapeutic Strategy for Acute Heart Failure. *Circ-Heart Fail.* **4**, 770–778